RCA

ESD ACCESSION LIST
ESTI Call No. __AL 48716__
Copy No. __/__ of __/__ cys.

# DEVELOPMENT OF A LARGE DYNAMIC RANGE TUNNEL DIODE AMPLIFIER FOR PHASED ARRAY RECEIVERS

## FINAL REPORT

1 January to 30 September 1965
Contract No. AF 19(628)-500
Subcontract No. 305

*prepared for*

## LINCOLN LABORATORY

### MASSACHUSETTS INSTITUTE OF TECHNOLOGY
### LEXINGTON, MASSACHUSETTS
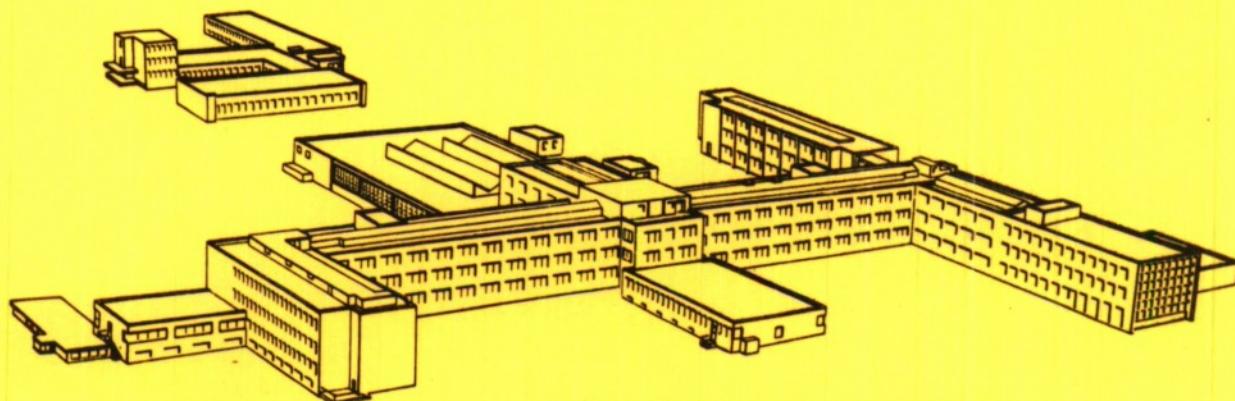
ESRL

AD626224

# DEVELOPMENT OF A LARGE DYNAMIC RANGE TUNNEL DIODE AMPLIFIER FOR PHASED ARRAY RECEIVERS

## FINAL REPORT

1 January to 30 September 1965

Contract No. AF 19(628)-500

Subcontract No. 305

*prepared for*

## LINCOLN LABORATORY

### MASSACHUSETTS INSTITUTE OF TECHNOLOGY

### LEXINGTON, MASSACHUSETTS

**RCA**

| Prepared by: | Approved by: |
|---|---|
| A.Presser | F.Sterzer |

## ABSTRACT

The objective of this two-phase program was to develop large dynamic range S-band tunnel diode amplifiers for phased array receivers. Under phase I a prototype amplifier was developed and subsequently delivered to Lincoln Laboratories. Phase II called for a reproducibility study of these amplifiers, and for the investigation of amplifier characteristics pertinent to phased array applications.

This report covers the experimental work performed under phase II and the results that were obtained in reproducing three amplifiers. Also, for completeness of this report, parts of the theoretical work performed during phase I are included.

Three two-stage tunnel diode amplifiers were delivered to Lincoln Laboratories in fulfillment of the phase II requirements. These amplifiers operate at a center frequency of 2.85 Gc/s $\pm 2\%$, have a 1.5 dB bandwidth ranging from 400-450 Mc/s at a gain of 18.0 to 18.5 dB, and have a noise figure between 5.6 and 5.9 dB. The amplifiers are unconditionally stable, and their output power at the 1 dB compression point ranges from -10.5 dBm to -12 dBm. The phases of any two amplifiers track within $\pm 3^{\circ}$ over a band of 110-190 Mc/s, and the amplitudes track within $\pm 1/2$ dB over a band of 290-410 Mc/s.

ii.

## TABLE OF CONTENTS

## LIST OF FIGURES

## LIST OF FIGURES

# LIST OF FIGURES

## 1.0  Introduction

Conventional low noise tunnel diode amplifiers using either gallium antimonide or germanium tunnel diodes have a power output at the 1 dB gain compression point of about -27 dBm and -24 dBm, respectively. The resulting dynamic range of these amplifiers is inadequate for most phased array receivers.  The aim of this program was to increase the dynamic range of tunnel diode amplifiers so that they can be considered for phased array applications.

The two-phase program called specifically for the development of tunnel diode amplifiers with the following objective performance:

| | | |
|---|---|---|
| 1. | Center Frequency | 2.85 Gc/s |
| 2. | 1.5 dB Bandwidth | 15% (425 Mc/s) |
| 3. | Gain | 17 dB min. |
| 4. | Noise Figure | 6 dB max. |
| 5. | Power Output (at 1 dB gain Compression) | -10 dBm min. |
| 6. | Input Match | 2:1 max. |
| 7. | Output Match | 1.3:1 max. |
| 8. | Stability | unconditional |
| 9. | Size | 1.7 $\lambda$ max. |
| 10. | Connectors | N-female |
| 11. | Amplitude Tracking | $\pm 1/2$ dB over 10% band |
| 12. | Phase Tracking | $\pm 3^{\circ}$ over 10% band |
| 13. | RF Overload | 50 mW   CW |
| 14. | Temperature | $10^{\circ}$-$30^{\circ}$ C |
| 15. | Reliability | $10^{4}$ hours |

This report covers in Section 2 the theoretical problem of obtaining large power outputs from tunnel diode amplifiers. General tunnel diode amplifier characteristics are considered in Section 3. Amplifier design and selection of its associated components are discussed in Section 4. Test methods and the results that were obtained on three experimental amplifiers are shown in Section 5. Concluding remarks and recommendations are given in Section 6.

## 2.0 Large Dynamic Range Tunnel Diode Amplifiers

### 2.1 Outline of Analysis

In the usual small signal analysis of tunnel diode amplifiers it is always assumed that the junction conductance of the diode is independent of the rf amplitude. Thus, the small signal gain of the amplifier is constant.

In the present analysis the dependence of the junction conductance is taken into account. The I-V characteristic of the tunnel diode is approximated by a tenth order power series and the coefficients of this series are used to define an effective large signal junction conductance $(G_d)_e$ at the fundamental input frequency. Graphical methods reduce the analysis of the amplifier from a non-linear to a linear problem. For small gain depressions (up to 3 dB) a closed form expression for input and output power under dynamic conditions is derived.

## 2.2 Large Signal Analysis of Tunnel Diode Amplifiers

Fig. 1 shows a schematic of a circulator-coupled reflection type tunnel diode amplifier. An equivalent circuit of this amplifier, assuming an ideal circulator, is shown in Fig. 2. In this circuit the diode is represented by its equivalent circuit [1] consisting of the junction conductance $(G_d)_e$, shunted by the junction capacitance C, both in series with the parasitic inductance L and resistance r. The amplifier circuit is represented by the susceptance $B_c$ and the circuit losses $G_c$.

The power gain G of such an amplifier is:

$$G = |\Gamma|^2 = \frac{(G_o + G_t)^2 + B_t^2}{(G_o - G_t)^2 + B_t^2} \tag{1}$$

where $\Gamma$ is the voltage reflection coefficient, $G_o$ is the circulator admittance, and $G_t$ and $B_t$ are the total negative conductance and total susceptance, respectively, across the circulator conductance.

In general, Eq. 1 is difficult to evaluate since both total $G_t$ and total $B_t$ are functions of frequency and rf-amplitude. It should be noted that the maximum gain does not necessarily occur where $B_t(f) = 0$, which can be verified by taking the frequency derivative of Eq. 1. The simplest solution of Eq. 1 is obtained by assuming that the circuit is lossless ($G_c = 0$) and that the series parasitics of the diode can be neglected ($r = L = 0$). Under these assumptions the power gain at resonance is maximum and can be written as:

$$G = \frac{\left[G_o + (G_d)_e\right]^2}{\left[G_o - (G_d)_e\right]^2} \tag{2}$$

In order to calculate the gain as given by either Eq. 1 or Eq. 2 the dependence of $(G_d)_e$ on the amplitude of the rf-voltage appearing across the diode junction has to be found. This dependence was calculated for a typical Ge and GaAs tunnel diode by the use of the following tenth-degree power series approximation of their I-V characteristics:

$$I_d = \sum_{n=0}^{10} a_n \, (V_d)^n \tag{3}$$

Eq. 3 is plotted in Fig. 3 together with the measured I-V characteristics of a typical Ge and GaAs tunnel diode normalized to the diode peak current $I_p$.

If the rf-component of $V_d$, the voltage across the diode junction, is assumed to be purely sinusoidal and represented by $V_o \cos \omega t$ then:

$$V_d = V_b + V_o \cos \omega t \tag{4}$$

where $V_b$ is the bias voltage and $V_o$ the peak rf voltage. Then

$$I_d = \sum_{n=o}^{10} a_n \, (V_b + V_o \cos \omega t)^n \tag{5}$$

$$= I_o + I_1 \cos \omega t + \text{(Harmonic terms)}.$$

The dynamic junction conductance $(G_d)_e$ at the fundamental frequency is then defined as:

$$(G_d)_e = \frac{I_1}{V_o} \tag{6}$$

In the limit of vanishingly small rf signals the value of the junction con-
ductance is given by the slope of the I-V characteristics at the bias point,
thus:

$$(G_d)_o = \frac{dI_o}{dV_b} \tag{7}$$

where $I_o$ is the dc current through the diode. Depending upon the particular
amplifier application, the bias point is chosen near the point where the
negative junction conductance is maximum. For the typical tunnel diodes
with characteristics as shown in Fig. 3:,

$$(G_d)_{max} = \frac{I_p}{0.11} \qquad \text{for Ge}$$

$$\tag{8}$$

$$(G_d)_{max} = \frac{I_p}{0.22} \qquad \text{for GaAs}$$

where $I_p$ is the diode peak current in amperes. Fig. 4 shows a normalized
plot of $(G_d)_o$ vs. the reduced bias voltage $\frac{V_b}{V_p}$ where $V_p$ is the bias voltage
corresponding to the peak current $I_p$. The calculated values of the effective
junction conductance ratio $\mathfrak{G}$ , defined by:

$$\mathfrak{G} = \frac{(G_d)_e}{(G_d)_o} , \tag{9}$$

as a function of $V_o/V_p$ is plotted in Fig. 5 for three different bias
voltages. The three curves shown are for a bias $V_{b_m}$ where $(G_d) = (G_d)_{max}$,
for a bias $V_{b_n}$ where the noise voltage $I_o(R_d)_o$ is minimum, and for a bias

$V_b{}_f$ where $(G_d)_e$ vs. $V_o/V_p$ is maximally flat.   Also shown in Fig. 5 is the gain depression $\Delta G$ in dB as a function of $\sigma$ for various maximum gain values.   This maximum gain value at resonance can be found from Fig. 6, where the maximum gain is plotted as a function of the load ratio $\alpha'$ defined as:

$$\alpha' = \frac{G_o}{(G_L)_o} \qquad (10)$$

where $G_o$ is the load conductance and $(G_L)_o$ the absolute value of the small signal load conductance.   For the lossless case ($n = L = 0$) the load ratio is:

$$\alpha = \frac{G_o}{(G_d)_o} \qquad (10a)$$

The power relation of a lossless reflection type amplifier is:

$$P_{out} = P_{in} + P_d \qquad (11)$$

where $P_{in}$ is the input power to the amplifier and $P_d$ is the power generated by the negative conductance of the diode junction.   The power generated by the diode is

$$P_d = \frac{V_o{}^2}{2} (G_d)_e \qquad (12)$$

Also

$$P_{out} = G \, P_{in} \qquad (13)$$

so that

$$P_{in} = \frac{V_o^2}{2} \, (G_d)_e \, \frac{1}{(G-1)} \tag{14}$$

$$P_{out} = \frac{V_o^2}{2} \, (G_d)_e \, \frac{1}{1-\frac{1}{G}} \tag{14a}$$

Eq. 14 can be solved graphically by means of Fig. 5. For small gain compressions (or more specifically for $1 \gg \sigma \gg .55$) the $\sigma$ vs. $V_o/V_p$ curve of Fig. 5 can be approximated by the following expression:.

$$\sigma = 1 - bV_o^2 \tag{15}$$

where

$$b = \begin{cases} .094 \text{ for } V_{bm} \\ .033 \text{ for } V_{bn} \\ .018 \text{ for } V_{bf} \end{cases}$$

Using the definitions of $\alpha$ and $\sigma$ the gain is given by:

$$G = \left[ \frac{\alpha + \sigma}{\alpha - \sigma} \right]^2 \tag{16}$$

and the maximum gain $G_{max}$ (for practical bias voltages $V_b$ where $\sigma \leq 1$ for all rf-amplitudes) by:

$$G_{max} = \left[ \frac{\alpha + 1}{\alpha - 1} \right]^2 \tag{16a}$$

Eq. 14 can be rewritten in closed form as:

$$P_{in} = \frac{(G_d)_o}{8b\alpha} \ (1 - \sigma)(\alpha - \sigma)^2 \qquad (17)$$

The saturation characteristics of a Ge tunnel diode amplifier and a GaAs tunnel diode amplifier, each biased at $V_{b_m}$, and each with 9 dB maximum gain, were calculated. It was assumed that both amplifiers employ a diode with $(G_d)_{max}$ = 36.4 mS (corresponding to a 4 mA Ge or a 8 mA GaAs diode) and the same load conductance $G_o$. The results of these calculations are plotted in Fig. 7. Also shown in this figure is the saturation character- istic of the cascade of these two amplifiers (Ge stage followed by GaAs stage) resulting in a maximum gain of 18 dB. Such a cascade was selected so as to result in a lower noise figure. For comparison, the saturation characteristics of single stage amplifiers with 18 dB gain of both Ge and GaAs tunnel diodes were calculated, using the same diodes as above with the load impedance changed to give 18 dB gain. The results are plotted in Fig. 8. From Figs. 7 and 8 it can be seen that the power output at the 1 dB gain compression point of the cascaded amplifier is 2.5 dB and 8.5 dB larger than for a single stage GaAs or Ge tunnel diode amplifier, respectively. It should be noted that the power output of a practical amplifier ($r \neq 0$, $L \neq 0$), using the same peak current diode, is less than the values that were calculated in this example.

The more general case, taking diode and circuit losses into ac- count, is treated in Ref. 2.

## 3.0   Tunnel Diode Amplifier Characteristics

### 3.1   Stability

The question of amplifier stability when using tunnel diodes is of greatest importance.  The tunnel diode exhibits a negative resistance up to the cutoff frequency $f_c$ defined as: [3]

$$f_c = \frac{(G_d)_o}{2\pi C} \left( \frac{1}{r(G_d)_o} - 1 \right)^{1/2} \tag{18}$$

where $(G_d)_o$, C, and r are defined as before.  In order to avoid unwanted oscillations the amplifier has to be stable for all frequencies up to $f_c$. If a diode has parameters such that:

$$\frac{L(G_d)_o}{r \ C} < 1 \tag{19}$$

then the terminal impedance of the diode is capacitive for all frequencies up to the cutoff frequency.  A diode obeying  Eq. 19 is sometimes referred to as short circuit stable.  In order to resonate such a diode the circuit reactance must be inductive, since the terminal impedance is capacitive for all frequencies up to $f_c$.  Using the circuit model of Fig. 2 the admittance to the left of the diode terminals 2-2 is then of the form $(G_o + G_c) - \frac{1}{j \ \omega L_c}$ (assuming lumped circuit elements).  A stability model that will be used subsequently is shown in Fig. 9.  The criteria for stability is that the roots of the characteristic equation:

$$Y_L(s) + Y_d(s) = 0 \tag{20}$$

are in the left half of the complex s-plane. The location of the roots
in the s-plane of Eq. 20 can be generally evaluated by the Routh criteria.[4]
For the given circuit the following relations of the physical constants
must be observed in order to assure stability:

$$\frac{L(G_d)^2_o}{C} < r(G_d)_o$$

$$(G_d)_o < \frac{(G_o + G_c)}{\frac{L_t}{L_c} + r(G_o + G_c)}$$

(21)

where $L_t = L + L_c$.

Eq. 21 expresses the relationship between the diode and circuit
parameters. It has been shown [5] that the general necessary and sufficient
conditions for stability are that:

$$\frac{L(G_d)^2_o}{C} < F(\theta)$$

$$r(G_d)_o < 1$$

(22)

where $3 > F(\theta) > 1$; $F(\theta)$ is a function of $r(G_d)_{max}$. Thus, for a given
set of diode parameters fulfilling Eq. 22 there exists a passive load ad-
mittance $Y_L(s)$, no matter how complicated to realize, that will stabilize
the tunnel diode. For the assumed load admittance $(G_o + G_c) - \frac{1}{j\omega L_c}$ and
diode parameters, Eq. 22 reduces to Eq. 21.

A graphical method to test stability of a given circuit is to plot the total passive admittance to the left of the fictitious diode junction terminal 1-1 (see Fig. 2) as a function of frequency on an admittance chart (say Smith chart). If the origin 0 of the chart is shifted by the amount $(G_d)_o /G_n$ to the right, where $G_n$ is the same normalizing constant used in the admittance plot, the criteria of stability is whether the plot encircles the new origin $0^1$ or not.[6] If the plot of Y encircles this origin then the circuit is unstable. A plot of a stable tunnel diode amplifier is shown in Fig. 10.

### 3.2 Gain

The gain of a reflection type tunnel diode amplifier is given by the absolute value of the power reflection coefficient and is thus given by Eq. 1.

$$G = \frac{(G_o + G_t)^2 + B_t^2}{(G_o - G_t)^2 + B_t^2} \tag{1}$$

Both $G_t$ and $B_t$ are generally functions of frequency and rf-drive and it is, therefore, not valid to assume that the maximum gain occurs at a frequency f where $B_t(f) = 0$. For a stable amplifier it can be shown that the maximum gain occurs at a higher frequency than the one for which $B_t = 0$. The frequency shift depends on the gain; if the gain increases the frequency shift decreases. The circulator admittance $G_o$ is in practice also a function of frequency, but its effect on the frequency shift in the pass band of the circulator is small.

### 3.3 Bandwidth

The maximum voltage gain bandwidth product obtainable from a single tuned reflection type tunnel diode amplifier under the most ideal circuit conditions ($r = L = G_c = 0$) and for a total circuit $Q > 2$ is given by:

$$G_v BW = \frac{(G_d)_{max}}{2\pi\ C} \frac{(\alpha + 1)}{\sqrt{1 - \frac{2}{G}}} \tag{23}$$

where $G_v$ is the voltage gain, BW is the 3 dB bandwidth, and the other parameters as defined in section 2. In practical circuits this gain bandwidth product is being reduced by the parasitic elements of the diode and by the frequency sensitivity of both circuit and circulator.

### 3.4 Noise Figure

The sources of noise in a tunnel diode amplifier are the shot noise of the tunnel diode and the thermal noise of the circuit and diode. The shot noise content , n, of tunnel diodes depends on the diode material and varies as: [7]

$$(n)_{GaSb} : (n)_{Ge} : (n)_{GaAs} = 1 : 1.75 : 2.35 \tag{24}$$

The noise figure of a tunnel diode amplifier for high gain and negligible circuit losses can be written as: [8]

$$F = \frac{1 + 20\ I_o/(G_d)_o}{\left[1 - r(G_d)_o\right]\left(1 - \frac{f^2}{f_c^2}\right)} \tag{25}$$

where $I_o$ is the dc-current through the diode at the bias point and $(G_d)_o$ the negative conductance at this point. The noise figures of typical S-band amplifiers, excluding circulator losses, are about 3.3 dB for GaSb, 4.3 dB for Ge and 5.3 dB for GaAs amplifiers.

### 3.5 Dynamic Range

The dynamic range is determined by the minimum detectable power, $P_{min}$, and usually by the power input at which gain compression is 3 dB, $(P_{in})_{3\ dB}$. Thus,

$$D = \frac{(P_{in})_{3\ dB}}{P_{min}} \tag{26}$$

$$P_{min} = KTBF \tag{27}$$

where K is Boltzmann's constant and T is the temperature in $^oK$. The gain compression is due to non-linearities of the I-V characteristic of the diode and has been discussed in section 2 of this report.

## 4.0  Tunnel Diode Amplifier Design

### 4.1 Tunnel Diode Selection

The choice of tunnel diode parameters depends on the required amplifier performance. Usually the gain, bandwidth, noise figure and dynamic range are specified. This information is sufficient for proper diode selection. For stability reasons it is desirable to select a diode with minimum series inductance L. The diode material is chosen either from noise figure or dynamic range considerations or a combination of both. The dynamic range requirements determine a peak current for the diode (Fig. 4 and Eqs. 14 and 16). The resulting diode conductance $(G_d)_{max}$ must fulfill the selected diode stability criteria (Eq. 19), the noise figure requirement (Eq. 25), and also result in a reasonably high cutoff frequency (Eq. 18). For low noise amplifiers the cutoff frequency is usually selected to be at least twice the operating frequency. From this additional requirement and the above equations the remaining diode parameters can be approximately determined. For large dynamic range amplifiers, which require high peak current diodes, it is increasingly important to use diodes with the smallest series inductance possible.

### 4.2 Circulator Selection

The circulator provides isolated input and output terminals for the amplifier and protects the tunnel diode amplifier module from mismatches at these terminals. The circulator is selected to have a minimum of insertion loss, a reasonable amount of isolation, and a low amplifier port VSWR over the amplifier bandwidth. If amplifiers have to be reproduced,

the impedance shape at the amplifier port has to be similar from unit to unit. Most present day four port circulators have a 10-20% bandwidth, an insertion loss of less than 0.3 dB, and isolations in excess of 25 dB. Temperature compensated circulators operating over the temperature range from -55°C to +70°C are also available.

### 4.3 Amplifier Circuit Design

The characteristic impedance of most commercial circulators is 50 ohms. The load impedance, for a specified gain, is determined by the load ratio $\alpha'$ and the dynamic range. For large dynamic range amplifiers the required load impedance is less than 50 ohms (about 10 ohms for the experimental amplifiers built). It is, therefore, necessary to transform the circulator impedance to the required impedance level. The amplifier port admittance of a practical circulator is not constant and real as previously assumed in the amplifier analysis. Figures 11A and 11B show the normalized admittance plots of two four port S-band circulators at the amplifier port, where the input and output ports were terminated in 50 ohms. Since the amplifier port VSWR at some frequencies can be very high, it is usually necessary to include a stabilizing network in the circuit so as to assure stability for all frequencies up to the cutoff frequency $f_c$ of the diode. [9] The circuit must also provide some means of tuning to the required center frequency. The diode must be stably dc biased into the negative resistance region, which requires a bias network. Fig. 12 is an equivalent circuit of a practical tunnel diode amplifier.

In this circuit $Y_c$ is the circulator admittance, the transmission line transformer is depicted by $\ell_1$, $Y_s$ is the admittance of the stabilizing circuit, $Y_t$ is the tuning susceptance, $C_B$ and $R_B$ are the elements of the bias network, and the tunnel diode is represented by its equivalent circuit.

The amplifier design can be checked by means of a stability plot similar to Fig. 10 (see also section 3.1). The admittance at the terminal 2-2 can be measured as a function of frequency, the known parasitic elements of the diode can be added, and the admittance $Y_{11}$ across the fictitious terminals 1-1 can be plotted. The stability can then be determined from a plot similar to Fig. 10 (see also section 3.1). If some instabilities occur (encircling of point 0') then the circuit has to be modified to avoid these instabilities. The stability plot using $G_n = (G_d)_o$ is also useful in determining the gain and the bandwidth of the amplifier at the terminals 1-1 by taking the square of the inverse reflection co-efficient $\Gamma^{-1}$ as obtained from the stability plot. If the circuit is lossless, then the gain G at terminals 3-3 is identical with the gain $(G)_{11}$ at the terminals 1-1. In the general case G is smaller than $(G)_{11}$ namely:

$$G = (G)_{11} \mid s \mid^2 \tag{28}$$

where $\mid s \mid < 1$ is the determinant of the scattering matrix of the passive network between the terminal pair 1 and 3.

## 5.0   Experimental Tunnel Diode Amplifiers

### 5.1   Design Considerations

The design and construction of the phase I amplifier was based upon the theoretical considerations presented in Section 2, Section 3, and Section 4.  These considerations made it apparent that a two stage amplifier is  the best solution to obtain the required dynamic range.  In the first stage a Ge tunnel diode was used and in the second stage a GaAs diode provided the large output power.  Each stage used a four port circulator.  These circulators were required to have similar amplifier port impedance characteristics (see Figs. 11A and 11B).  A sketch of the coaxial amplifier structure that was developed is shown in Fig. 13.  The phase I amplifier delivered to Lincoln Laboratories had the following performance:

| | |
|---|---|
| Center Frequency | 2.86 Gc/s |
| Gain | 17.3 dB |
| 1.5 dB Bandwidth | 120 Mc/s |
| Noise Figure | 5.6 dB |
| Power Output (at 1 dB gain compression point) | -13.7 dBm |
| Stability | unconditional |
| Spurious Output of IM products (Up to 1 dB gain compression point) | -41 dBm max. |
| Dynamic Range per Mc/s Receiver Bandwidth (to 3 dB compression) | 83.6 dB |

More details of this amplifier are given in the phase I final report. A photograph of one amplifier stage is shown in Fig. 14.

The objectives of the phase II program were:

    a.   To improve the amplifier developed under the phase I effort.

    b.   To reproduce and evaluate three of these improved amplifiers.

    c.   To investigate the tracking characteristics of any two of these amplifiers.

    d.   To deliver these amplifiers to Lincoln Laboratories upon completion of their evaluation.

The improvement program was started with a mechanical redesign of the amplifier structure. The stubs of the tuner and stabilizing circuit were rigidly supported in a solid aluminum structure. The same structure also removed some of the electrical discontinuities at the interface between the circulator and the amplifier module. In order to improve the bandwidth of the amplifier, ultra low height (.010") ceramic micro stud diode packages with a case capacitance of less than 0.4 pF (compared to 2 pF for the strip line package used in the phase I amplifier) were selected. Tunnel diodes in this package exhibit a self inductance of about 150 pH (compared to 75 pH for the strip line diode) but their greater mechanical strength and the possible increase of amplifier bandwidth favored their use. The excess series inductance of the diode within

the amplifier structure can also be reduced due to the favorable geometry of the package that allows minimization of diode mounting discontinuities. The bias section of the amplifier was redesigned, to accommodate the micro stud package, and also improved so as to reduce the possibility of rf-leakage. It was decided to use for the phase II two stage amplifier, a single six-port circulator in place of two four port circulators, which reduces the length of the amplifier by one inch. The amplifier port admittance shape in the pass band was specified to be similar from unit to unit with a maximum VSWR of 1.15.

The remaining amplifier circuit components were essentially the same as in the phase I amplifier, consisting of:

      a.  A transformer section designed to result in a gain of about 9 dB.

      b.  A variable short circuit tuner that also provides the dc return path for the diode.

      c.  A stabilizing circuit designed to have negligible loading in the pass band of the amplifier and to have sufficient loading elsewhere, in order to assure stability.

      d.  A dc bias network that bypasses the rf signal and permits establishment of a stable dc operating point in the negative resistance region of the diode.

The diodes, both Ge and GaAs, and the circulators used were made to the following specifications:

Tunnel Diodes:

$$(R_d)_{min} = 27 \text{ ohms} \pm 3\%$$

$$C_j = 2.3 \text{ pF} \pm 10\%$$

$$9 \geqslant \frac{(R_d)_{min}}{r} \geqslant 4.5$$

$$\frac{I_p}{I_v} \geqslant 10$$

Six-port Circulator:

| | |
|---|---|
| Frequency | 2.6-3.2 Gc/s |
| VSWR (all ports) | $\leqslant 1.15:1$ |
| Insertion Loss | $\leqslant 0.3$ dB per pass |
| Isolation (input) | $\geqslant 25$ dB |
| (output) | $\geqslant 40$ dB |

Amplifier port admittance shape in the pass band to be similar from unit to unit.

Fig. 15 shows a sketch of a single phase II amplifier structure and Fig. 16 is a photograph of a completed two stage amplifier.

## 5.2  Amplifier Performance

The performance of each amplifier (designated S128-21, S128-22 and S128-23) was evaluated.  The following characteristics were measured:

Gain versus frequency

Gain versus power input

1 dB gain compression output power versus frequency

Noise figure versus frequency

Gain versus insertion phase

Third and fifth order intermodulation cross products

power output versus power input.

Tracking performance of all three possible amplifier pairs was evaluated and the following characteristics were measured:

Amplitude tracking versus frequency

Phase tracking versus frequency

Phase tracking versus power input

The amplifiers were adjusted while using a swept frequency test set-up as shown in Fig. 17.  The bias of the first stage was set near the lowest noise voltage point of the diode and the bias of the second stage near the point of maximally flat power output.  The frequency response and the saturation characteristic were then measured by a point by point method using a calibrated signal source and a high sensitivity power meter.

The gain versus relative insertion phase test was performed in a set-up as sketched in Fig. 18; the signal is fed over a directional coupler which is terminated in a movable short circuit, a similar arrangement was at the amplifier output. The gain was recorded as the phase of the short circuit was continually shifted.

The noise figure of each amplifier was determined in a set-up as shown in Fig. 19 that permits automatic noise figure readings as well as by the Y-factor method.

The intermodulation cross products power output measurement was carried out by feeding two signals of equal amplitude but different frequency ($f_1$ and $f_2$) over a directional coupler to the amplifier. The frequencies $f_1$ and $f_2$ are spaced so that both signals and the third and fifth order cross products are within the pass-band of the amplifier. The amplitudes of the third order ($2 f_1 - f_2$ and $2 f_2 - f_1$) and fifth order ($3 f_1 - 2 f_2$ and $3 f_2 - 2 f_1$) cross product power were detected by a spectrum analyzer (see Fig. 20 for test arrangement).

Phase tracking was evaluated in a phase bridge as shown in Fig. 21. This phase bridge was initially balanced by applying a swept frequency signal at terminal 1 of the magic tee and by adjusting the level and phase of this signal in both arms of the bridge until a broad band null was observed at terminal 2 of the output magic tee. The phase difference of two amplifiers, one inserted in each arm, was recorded point by point as a function of frequency and as a function of power input for discrete frequencies.

The results of the above measurements on all three amplifiers delivered to Lincoln Laboratories are plotted in Fig. 22 through Fig. 47. The following is a listing of these plots:

Photograph of swept frequency response                 Fig. 22
   (S128-21, S128-22, and S128-23)

|  | Amplifier | | |
|---|---|---|---|
|  | S128-21 | S128-22 | S128-23 |
| Gain vs. frequency | Fig. 23 | Fig. 28 | Fig. 33 |
| Saturation characteristic | Fig. 24 | Fig. 29 | Fig. 34 |
| 1 dB gain compression vs. frequency | Fig. 25 | Fig. 30 | Fig. 35 |
| Gain vs. insertion phase | Fig. 26 | Fig. 31 | Fig. 36 |
| Third and fifth order IMC product power output vs. input power of each signal | Fig. 27 | Fig. 32 | Fig. 37 |

---

Typical noise figure vs. frequency                      Fig. 38

|  | Amplifier Pairs | | |
|---|---|---|---|
|  | S128-21 S128-22 | S128-21 S128-23 | S128-22 S128-23 |
| Amplitude tracking vs. frequency | Fig. 39 | Fig. 42 | Fig. 45 |
| Phase tracking vs. frequency | Fig. 40 | Fig. 43 | Fig. 46 |
| Phase tracking vs. input power | Fig. 41 | Fig. 44 | Fig. 47 |

The performance of these amplifiers can be summarized as follows:

| Amplifier | S128-21 | S128-22 | S128-23 |
|---|---|---|---|
| Center frequency (Gc/s) | 2.80 | 2.84 | 2.83 |
| Gain (dB) | 18.5 | 18.4 | 18.4 |
| 1.5 dB-Bandwidth (Mc/s) | 450 | 400 | 430 |
| Noise Figure (dB) | 5.9 | 5.7 | 5.6 |
| Power Output at 1 dB gain compression (dBm) | -11.4 | -11.3 | -10.6 |
| 3rd IMC-Signal output power ratio (dB) | | | |
| at 1 dB gain compression | 23.5 | 26.5 | 23.0 |
| at -45 dBm input | 40 | 41 | 32 |

| Amplifier Pair | S128-21 S128-22 | S128-21 S128-23 | S128-22 S128-23 |
|---|---|---|---|
| $\pm 3^{\circ}$ Phase tracking range (Mc/s) | 190 | 180 | 110 |
| $\pm 0.5$ dB Amplitude tracking range (Mc/s) | 290 | 310 | 410 |

## 6.0  Conclusion and Recommendations

It has been demonstrated that the dynamic range of tunnel diode amplifiers can be increased by about 14 dB.  This increase was accomplished by using high peak current tunnel diodes and by cascading two amplifiers of moderate gain.  The first stage of the amplifier incorporated  a Ge tunnel diode biased in the low noise region of its dc-characteristic, and in the second stage of the amplifier a GaAs tunnel diode was used dc-biased to give a large power output.  It also has been shown that these amplifiers can be reproduced with reasonable tolerances imposed upon diode parameters and circulator performance.  Three amplifiers were built and delivered to Lincoln Laboratories.  The performance of these amplifiers can be summarized as follows:

|  |  | Objectives |
|---|---|---|
| Center Frequency | 2.85 Gc/s $\pm$2% | 2.85 Gc/s |
| Gain | 17 dB min. | 17 dB min. |
| 1.5 dB-Bandwidth | 400 Mc/s min. | 450 Mc/s |
| Noise Figure | 6 dB max. | 6 dB max. |
| Power output at 1 dB gain compression | -11 dBm $\pm$0.5 dB | -10 dBm min. |
| $\pm 3^{\circ}$ Phase tracking range | 180 Mc/s $\pm$10% | 285 Mc/s |
| $\pm$0.5 dB Amplitude tracking range | 300 Mc/s $\pm$10% | 285 Mc/s |
| Size | 8 1/2 x 4 1/2 x 1 1/16 (1.2 $\lambda$ max. transverse) | 1.7$\lambda$ max. (transverse) |
| Weight | 2 lbs. 9 oz. max. | |

While the amplifiers constructed under this program operated at S-band frequencies, the techniques that were developed could be used to fabricate similar amplifiers up to at least X-band frequencies.

We also believe that significant improvements in both performance and size of these amplifiers are possible. First, the presently used six-port circulator uses permanent magnets and is therefore heavy and bulky. This circulator could be replaced by a magnetless, square loop lithium ferrite circulator. The weight and size of this circulator would be only a fraction of the presently used circulator, and since magnetless circulators can be readily switched, adjustment of multistage amplifiers would be greatly simplified. Second, the amplifier module could be fabricated by thin film integrated circuit techniques on the circulator circuit board. These techniques would reduce the parasitic series inductance of the diode, thus allowing the use of higher peak current diodes.

The above improvements would permit the construction of highly reproducible S-band tunnel diode amplifiers with excellent tracking characteristic. These amplifiers are expected to have a 25% bandwidth at a gain of 18 dB, a noise figure of 5 dB, and a power output of -6 dBm at the 1 dB gain compression.

References

1. H. S. Sommers, Jr., "Tunnel Diodes as High Frequency Devices", Proc. IRE, Vol. 47, July 1959.

2. R. Steinhoff and F. Sterzer, "Microwave Tunnel Diode Amplifiers with Large Dynamic Range", RCA Review, March 1964.

3. W. F. Chow, "Principles of Tunnel Diode Circuits", John Wiley & Sons, Inc., New York.

4. E. J. Routh, "Dynamics of Rigid Bodies", MacMillan, London.

5. L. I. Smilen and D. C. Youla, "Stability Criteria for Tunnel Diodes", Proc. IRE, Vol. 49, July 1961.

6. H. W. Bode, "Network Analysis and Feedback Amplifier Design", D. Van Nostrand Co., New York.

7. B. G. King and G. E. Sharpe, IEEE Transactions on ED, Vol. ED-11, Pg. 273, June 1964.

8. E. G. Nielsen, "Noise Performance of Tunnel Diodes", Proc. IRE, Vol. 48, November 1960.

9. J. Lepoff, "Design of Stable Broadband Tunnel Diode Amplifiers", Digest of 1964 PTGMTT International Symposium.
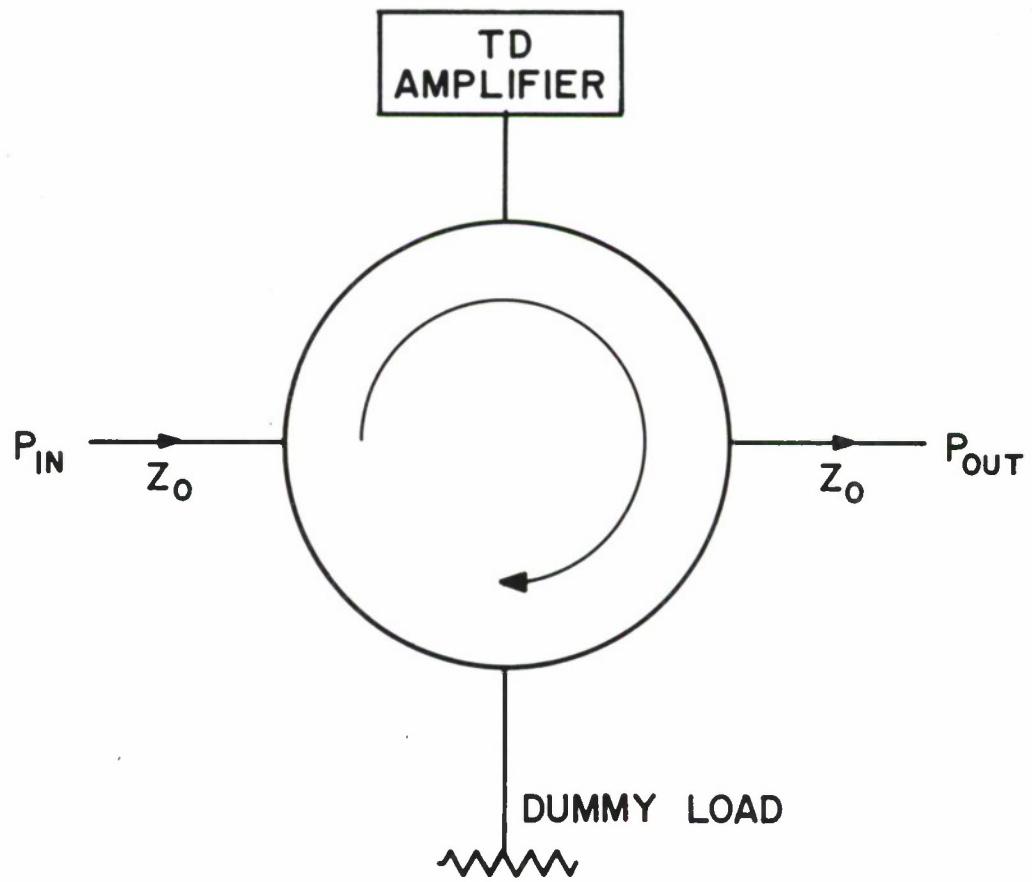
FIG.1. CIRCULATOR COUPLED TUNNEL
DIODE AMPLIFIER.
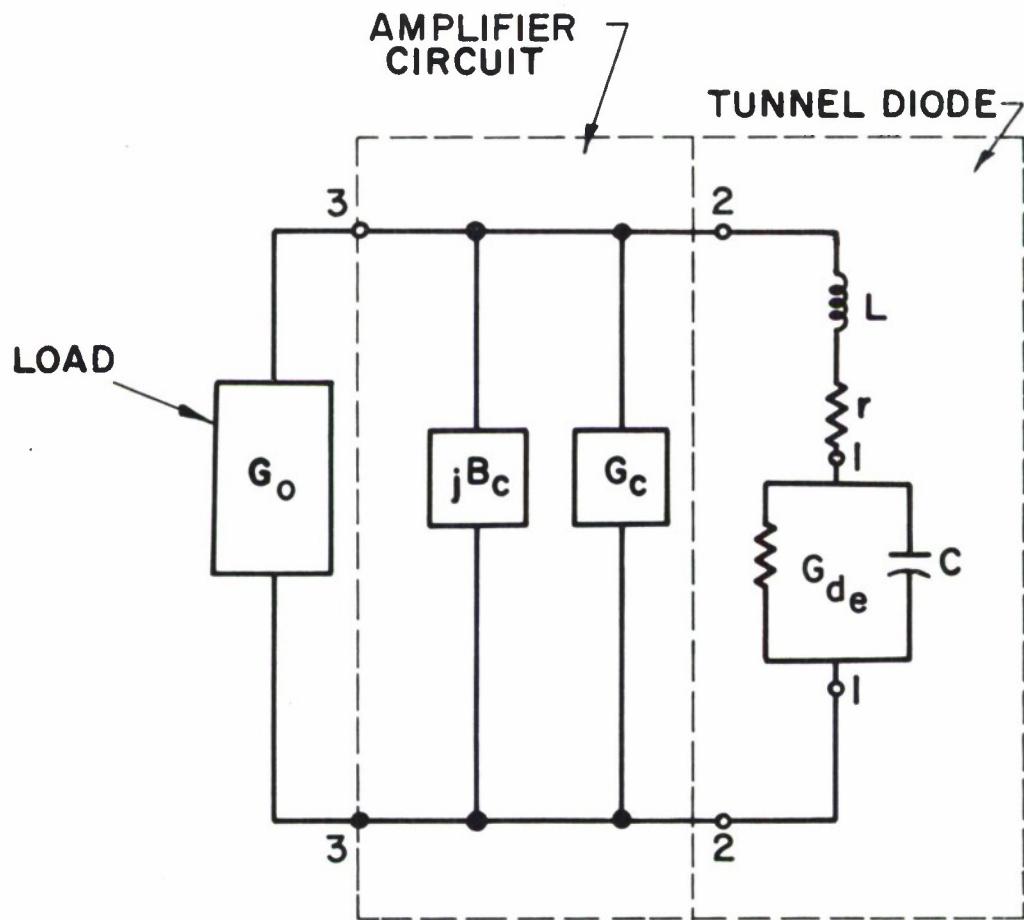
FIG. 2  EQUIVALENT CIRCUIT OF TUNNEL
DIODE AMPLIFIER
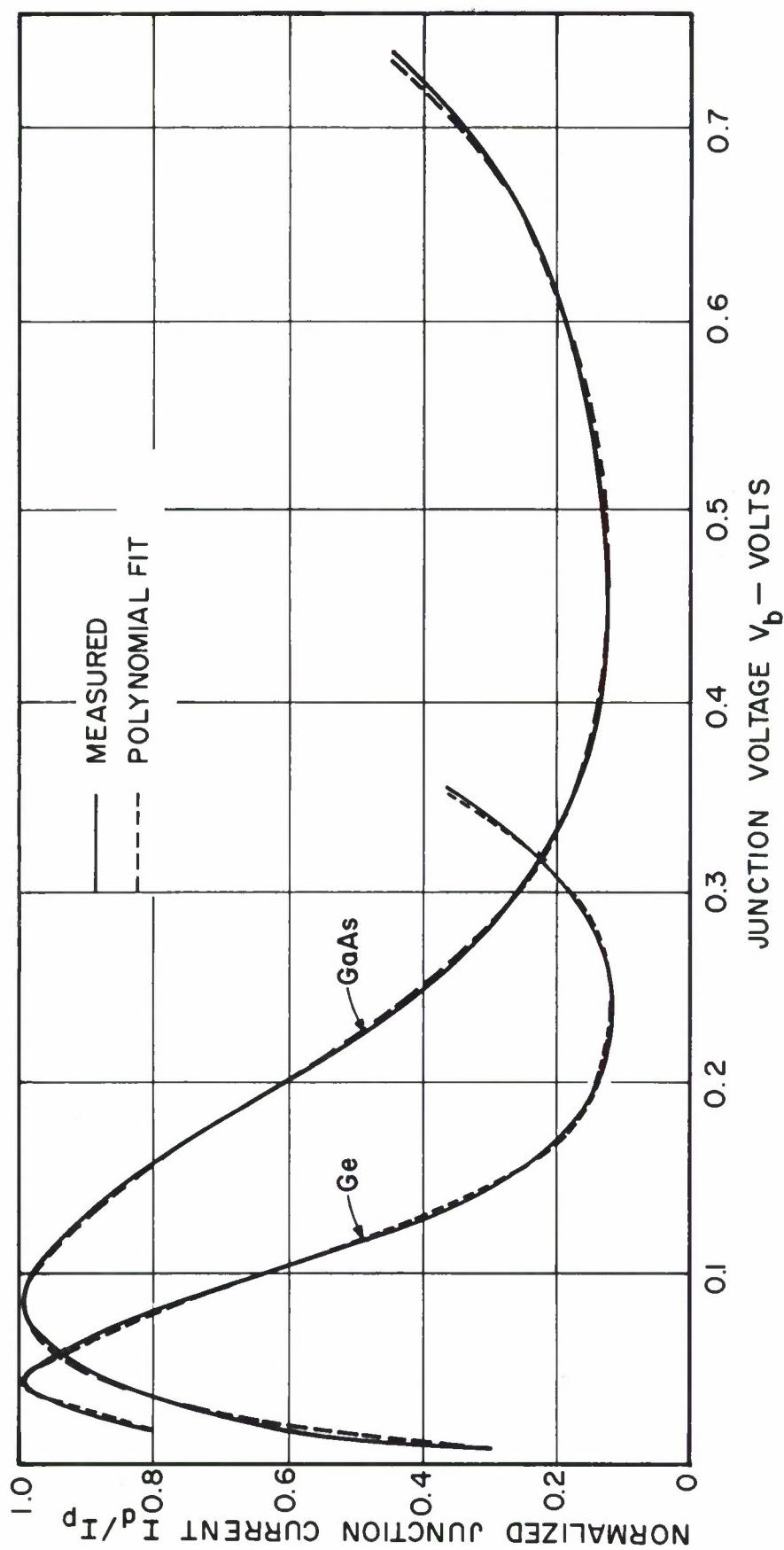
FIG.3. NORMALIZED I-V CHARACTERISTIC OF GaAs & Ge TUNNEL DIODE
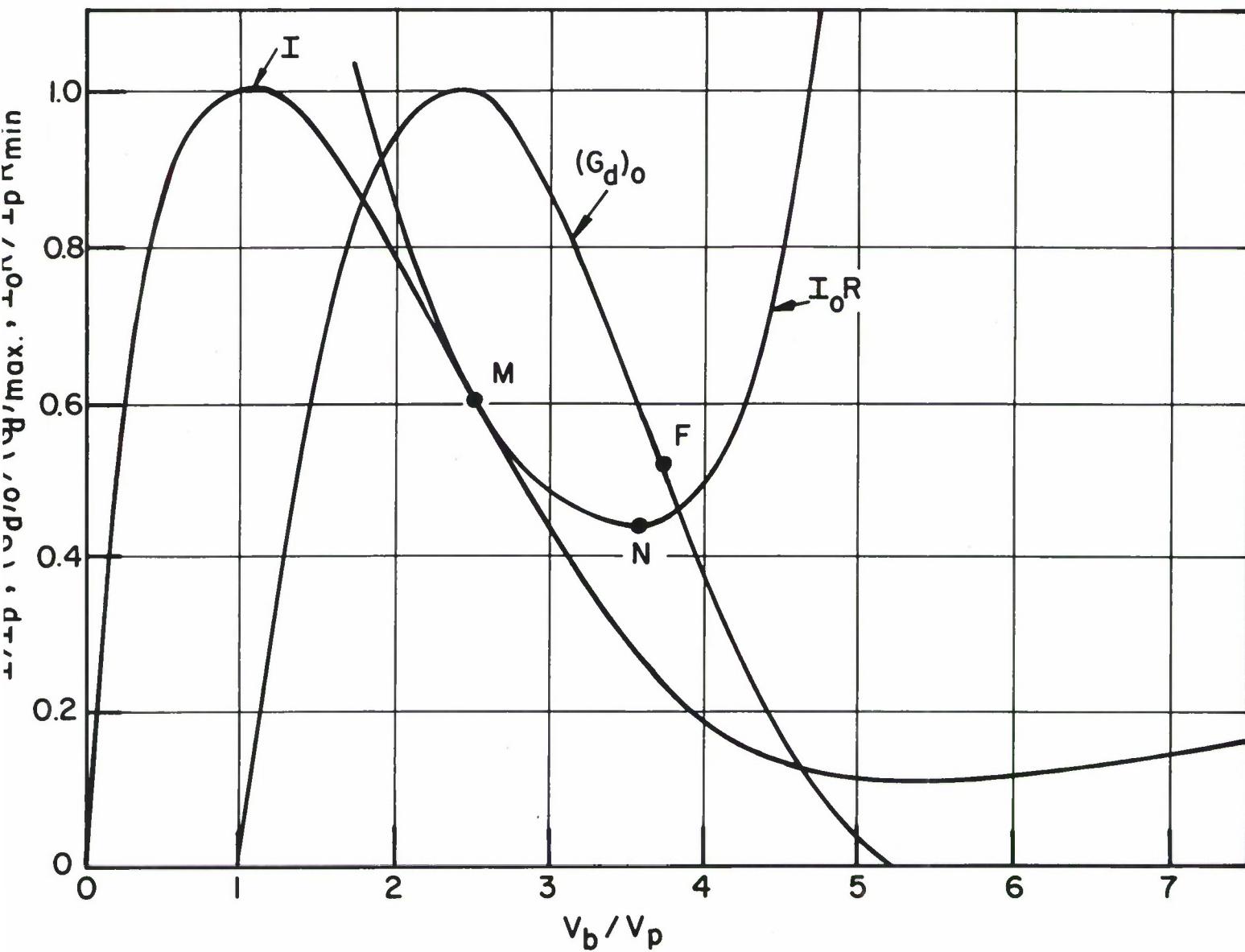
FIG. 4 NORMALIZED PLOT OF DIODE CURRENT,
JUNCTION CONDUCTANCE AND NOISE
VOLTAGE
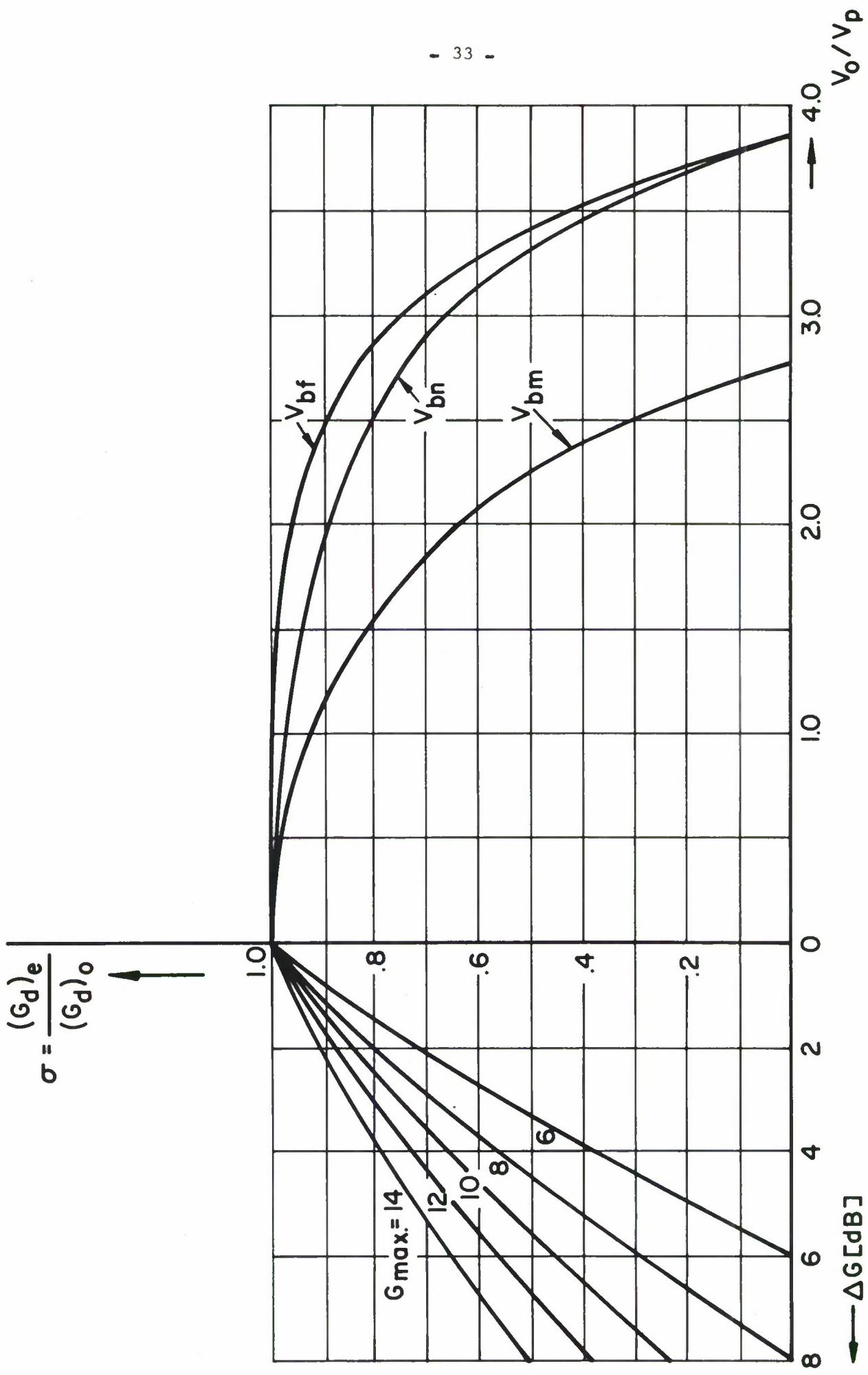
FIG. 5 EFFECTIVE JUNCTION CONDUCTANCE vs. RF VOLTAGE AMPLITUDE FOR
Ge AND Ga As TUNNEL DIODES
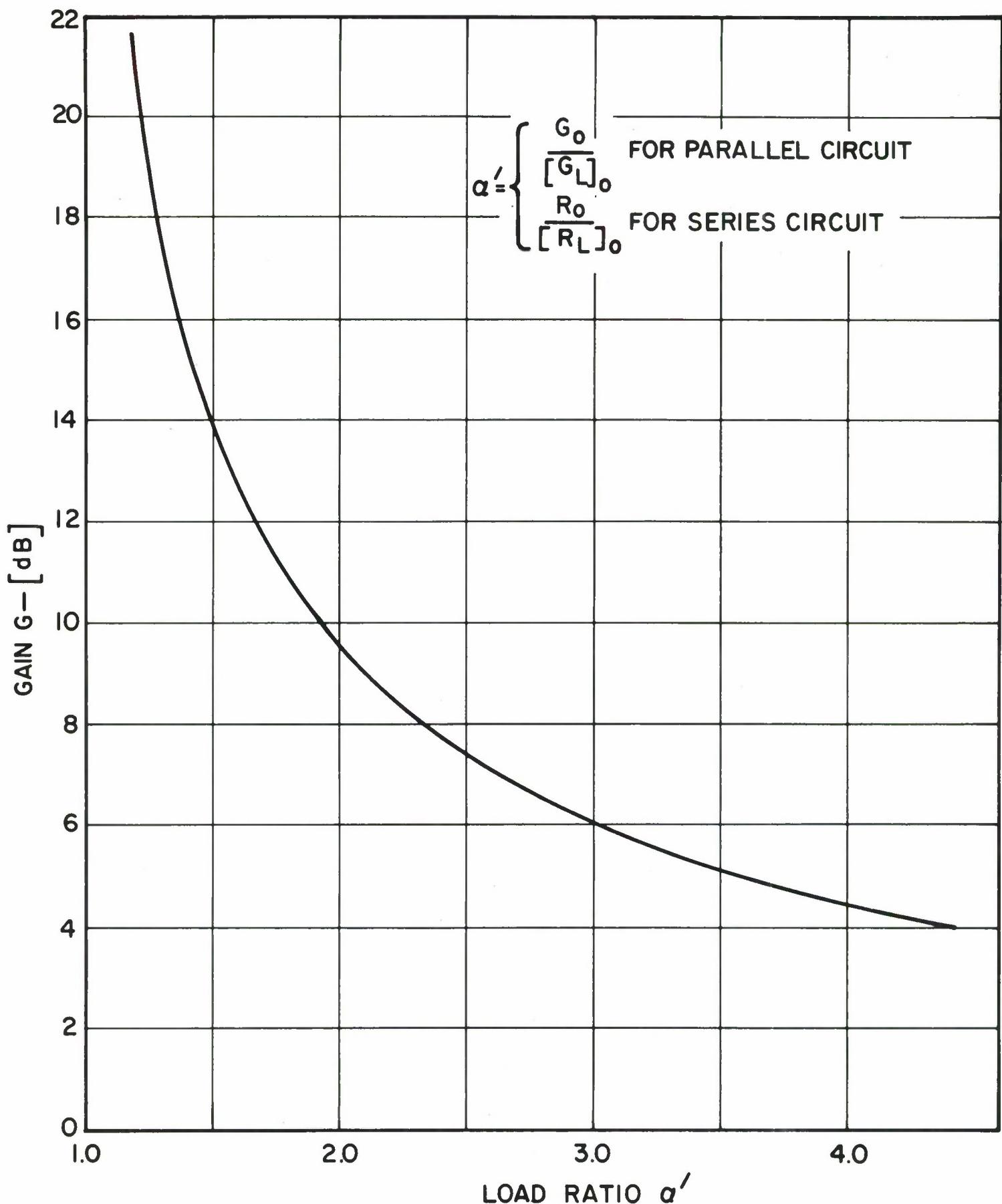
FIG. 6 GAIN vs. LOAD RATIO AT RESONANT FREQUENCY FOR CIRCU-
LATOR COUPLED TUNNEL-DIODE AMPLIFIER
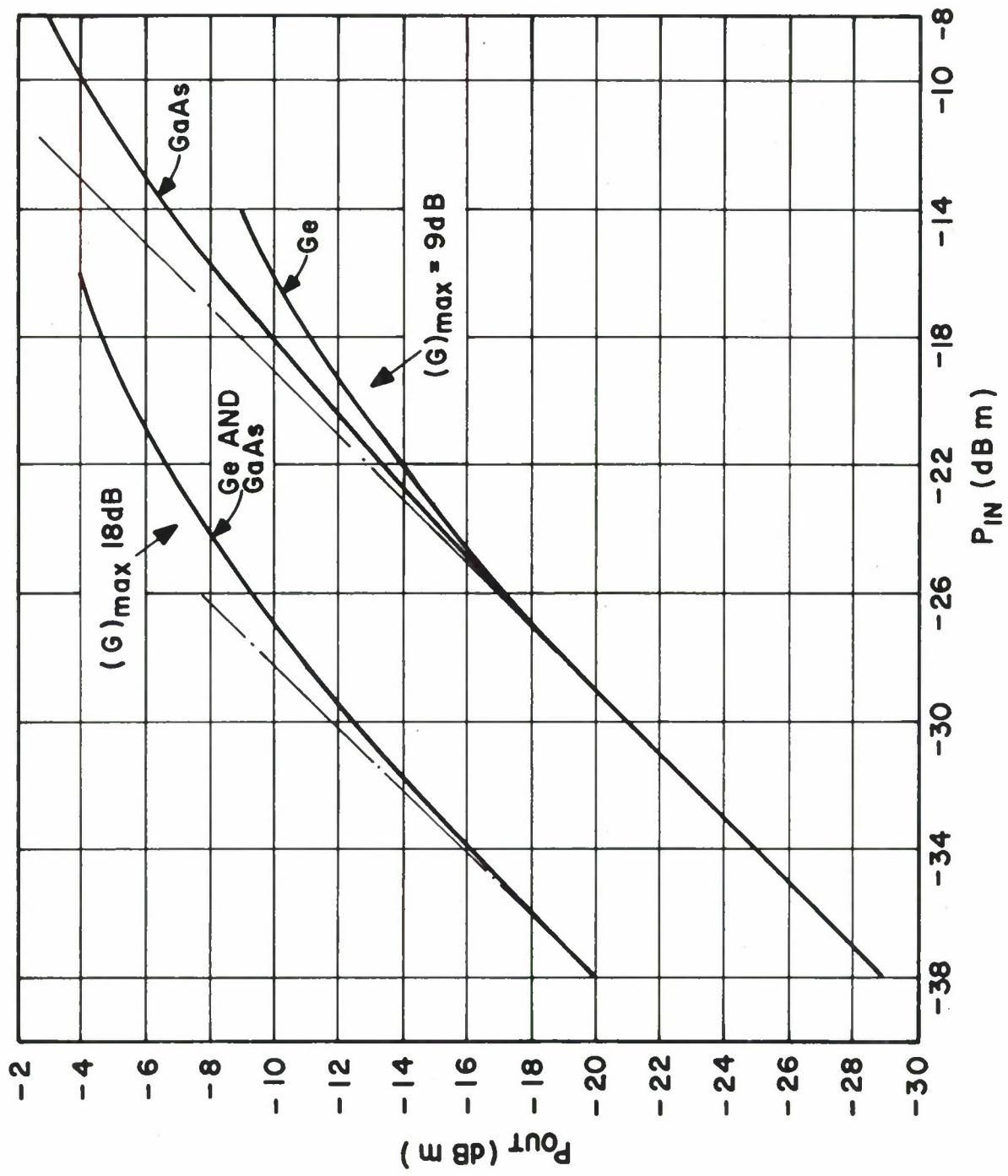
FIG.7. CALCULATED SATURATION CHARACTERISTICS OF Ge AND GaAs TUNNEL DIODE AMPLIFIERS.
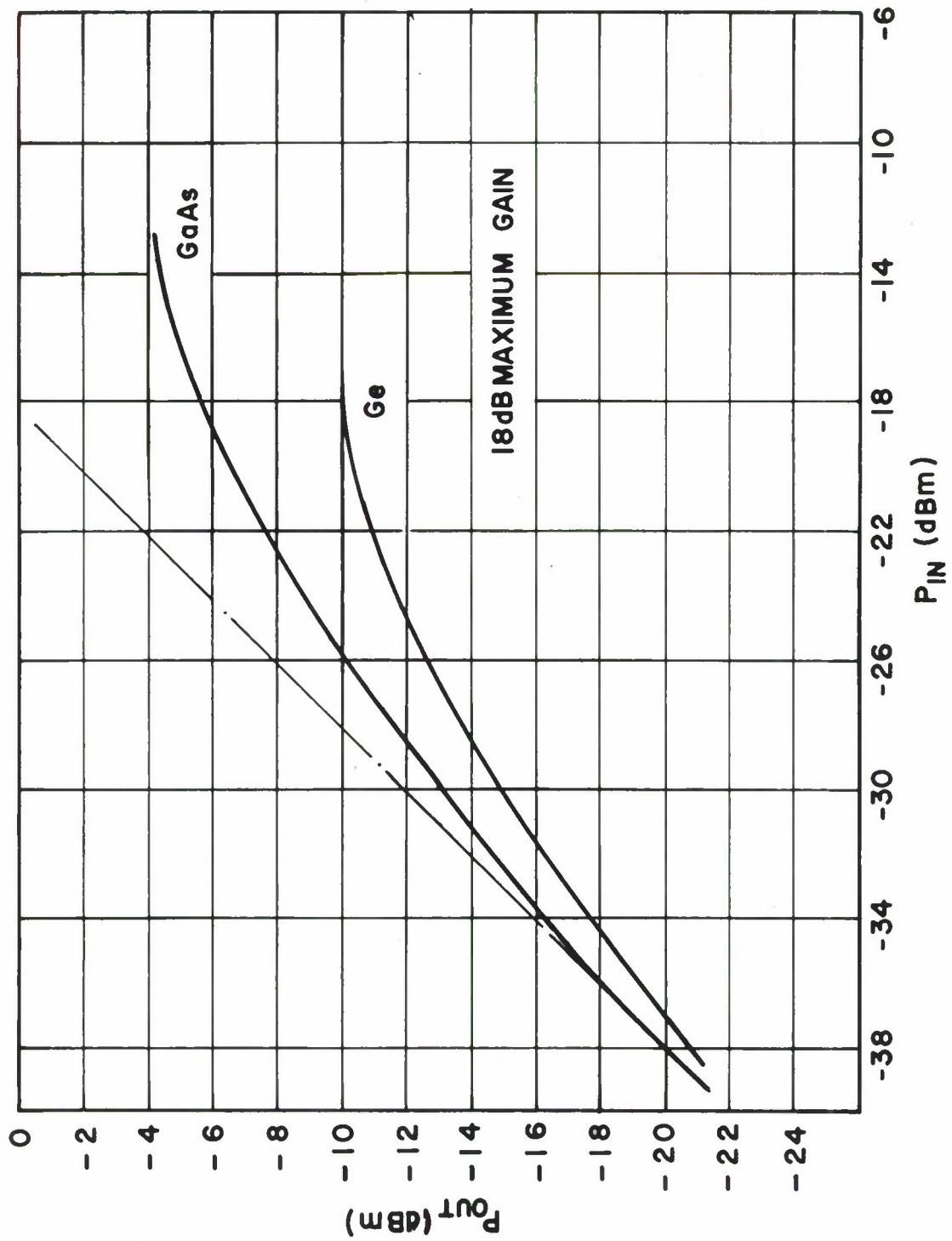
FIG.8. CALCULATED SATURATION CHARACTERISTICS OF SINGLE STAGE Ge AND GaAs TUNNEL DIODE AMPLIFIERS.

$$Y_{RESP.} = \frac{I_{IN}}{Y_{DIODE} + Y_{LOAD}}$$
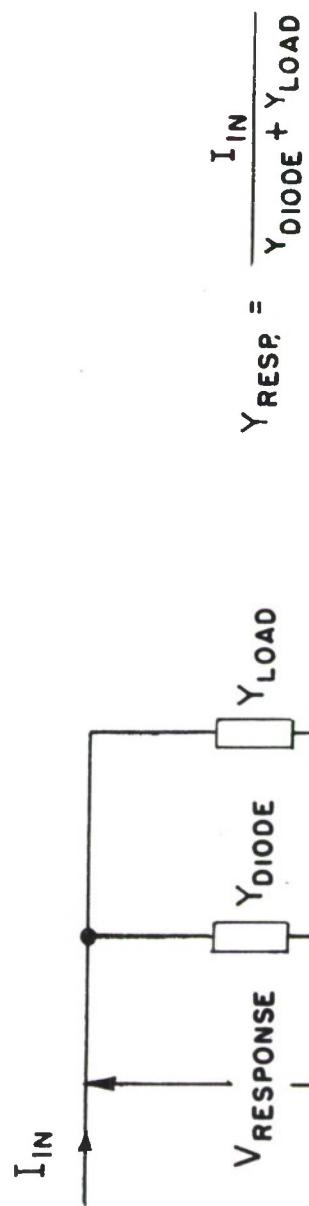
FIG. 9. STABILITY MODEL
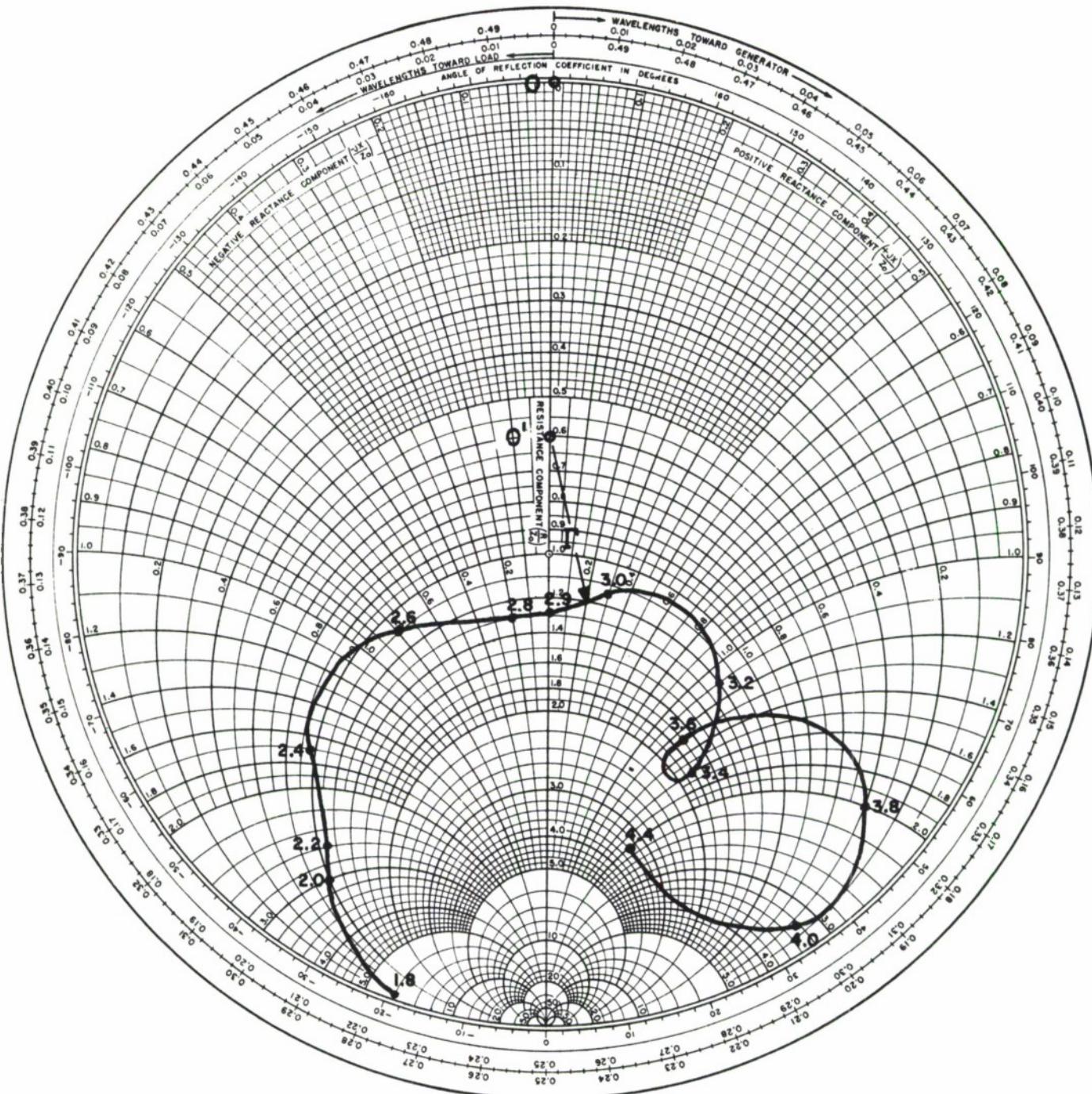
# FIG. 10. STABILITY PLOT OF A TUNNEL DIODE AMPLIFIER
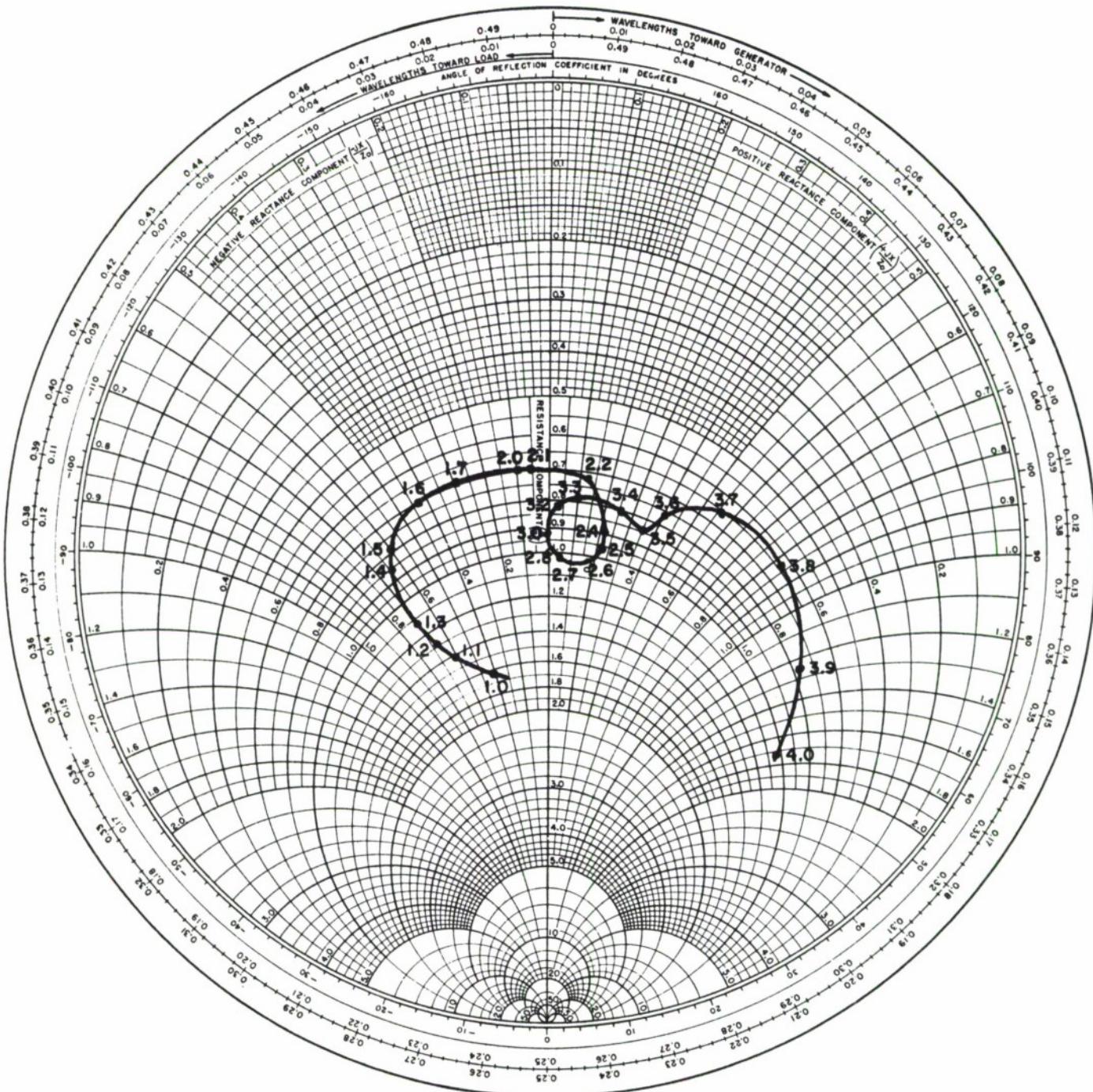
## FIG. 11A. NORMALIZED ADMITTANCE PLOT OF S-BAND CIRCULATOR.
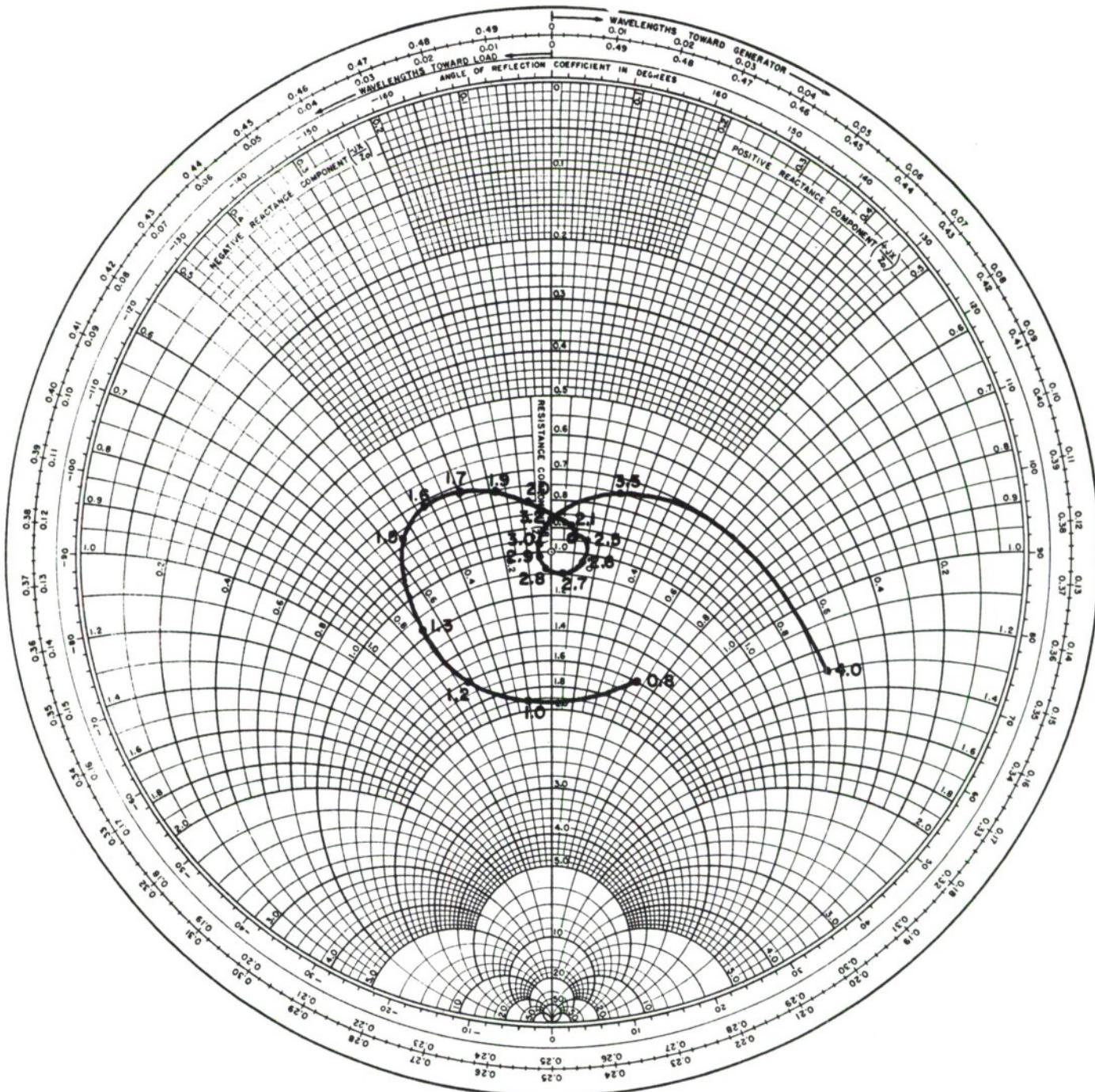
FIG.11B. NORMALIZED ADMITTANCE PLOT OF
S-BAND CIRCULATOR.
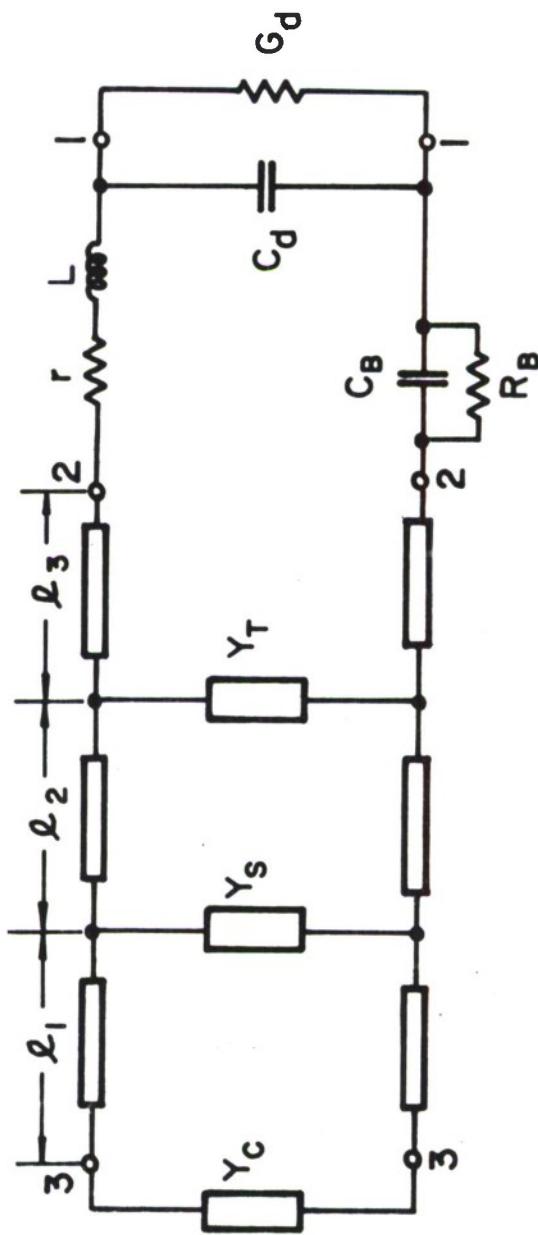
FIG. 12. EQUIVALENT CIRCUIT OF TUNNEL DIODE AMPLIFIER
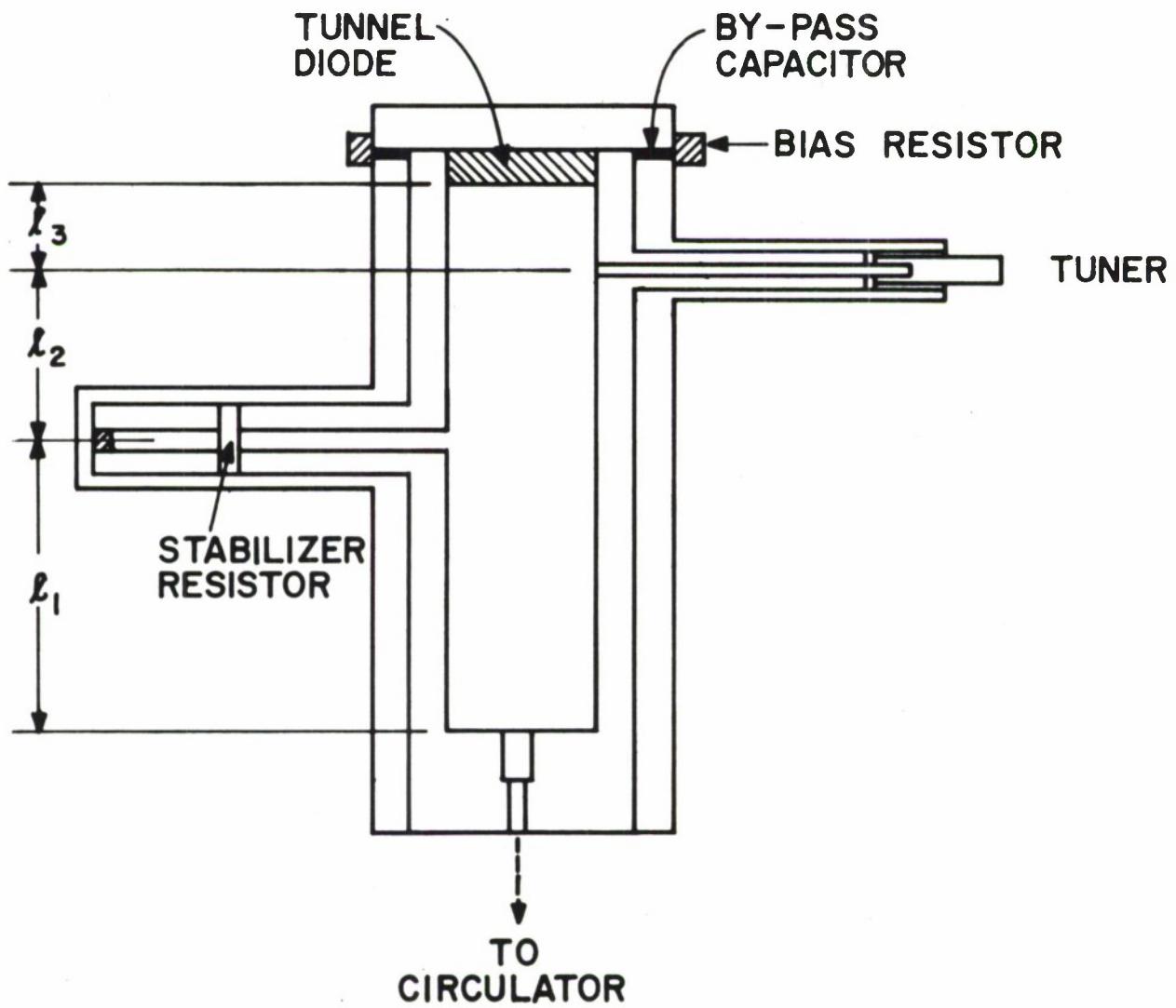
FIG. 13. S-BAND TUNNEL DIODE AMPLIFIER.

FIG.14. PHOTOGRAPH OF TUNNEL DIODE AMPLIFIER
( SINGLE STAGE )

BIAS TERMINAL

BIAS RESISTOR

VARIABLE TUNING CAPACITOR

BY-PASS
CAPACITOR

TUNNEL
DIODE

TUNER
SHORT CIRCUIT

VARIABLE CAPACITOR

STABILIZING RESISTOR

TO CIRCULATOR
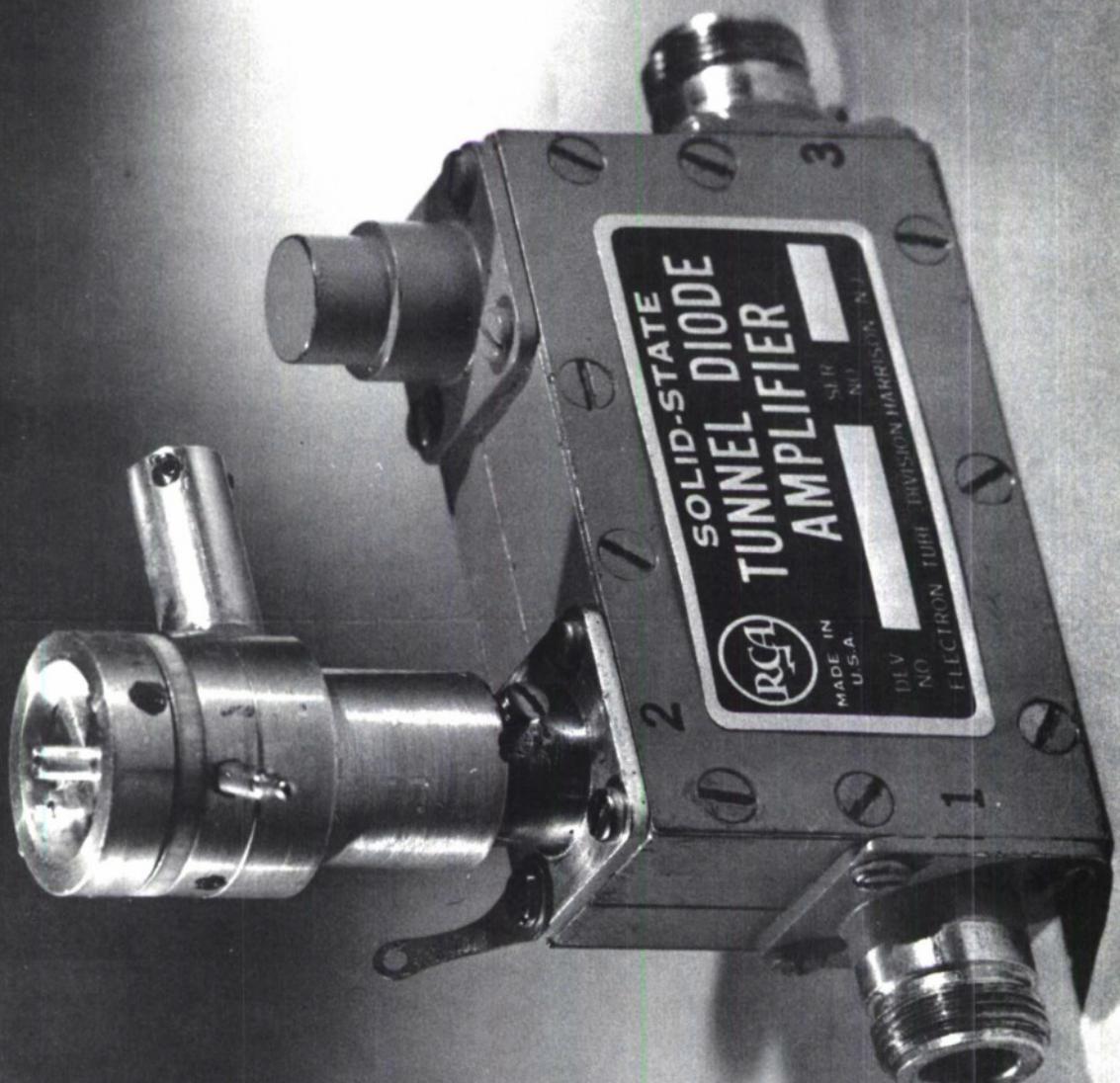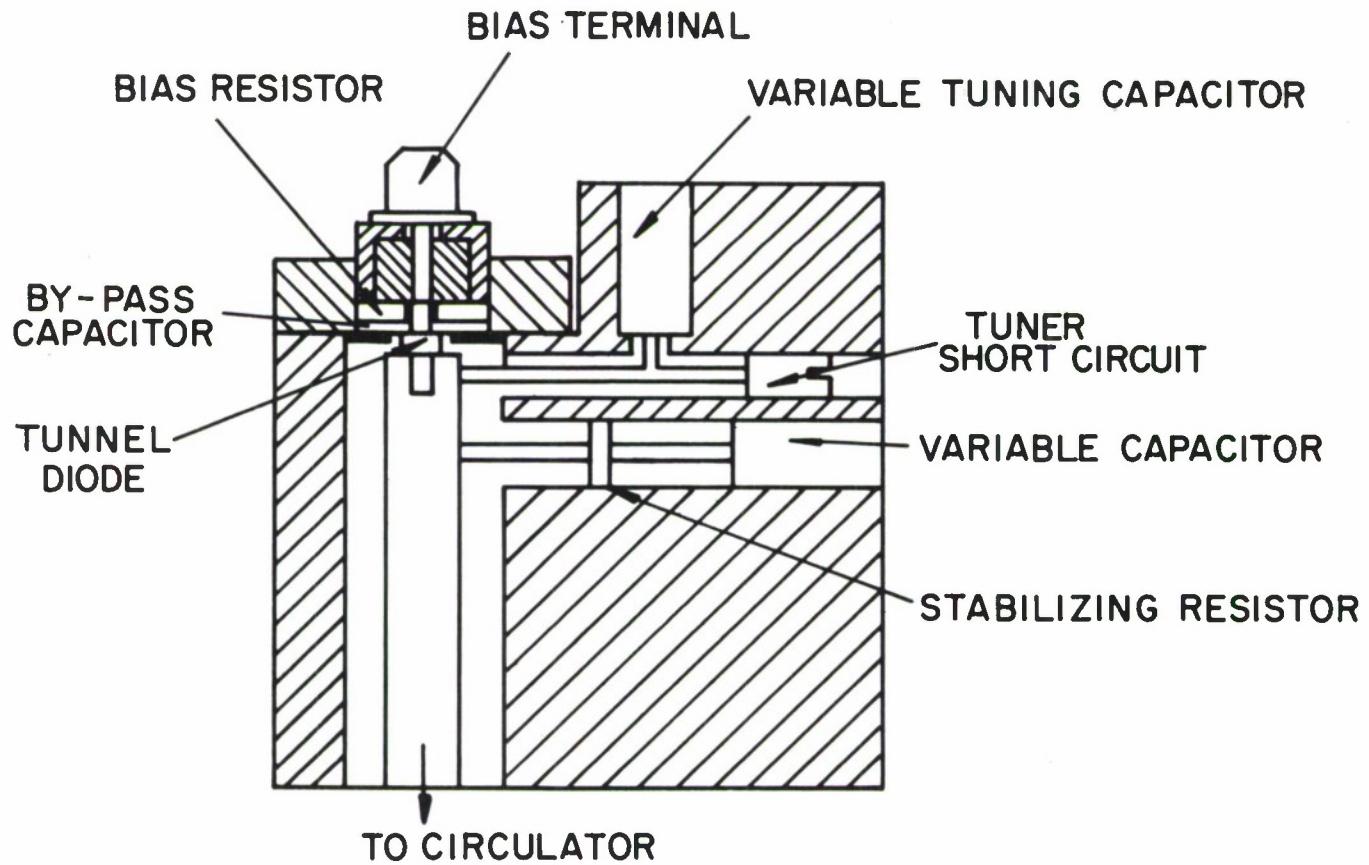
FIG. 15 PHASE II S-BAND TUNNEL DIODE AMPLIFIER
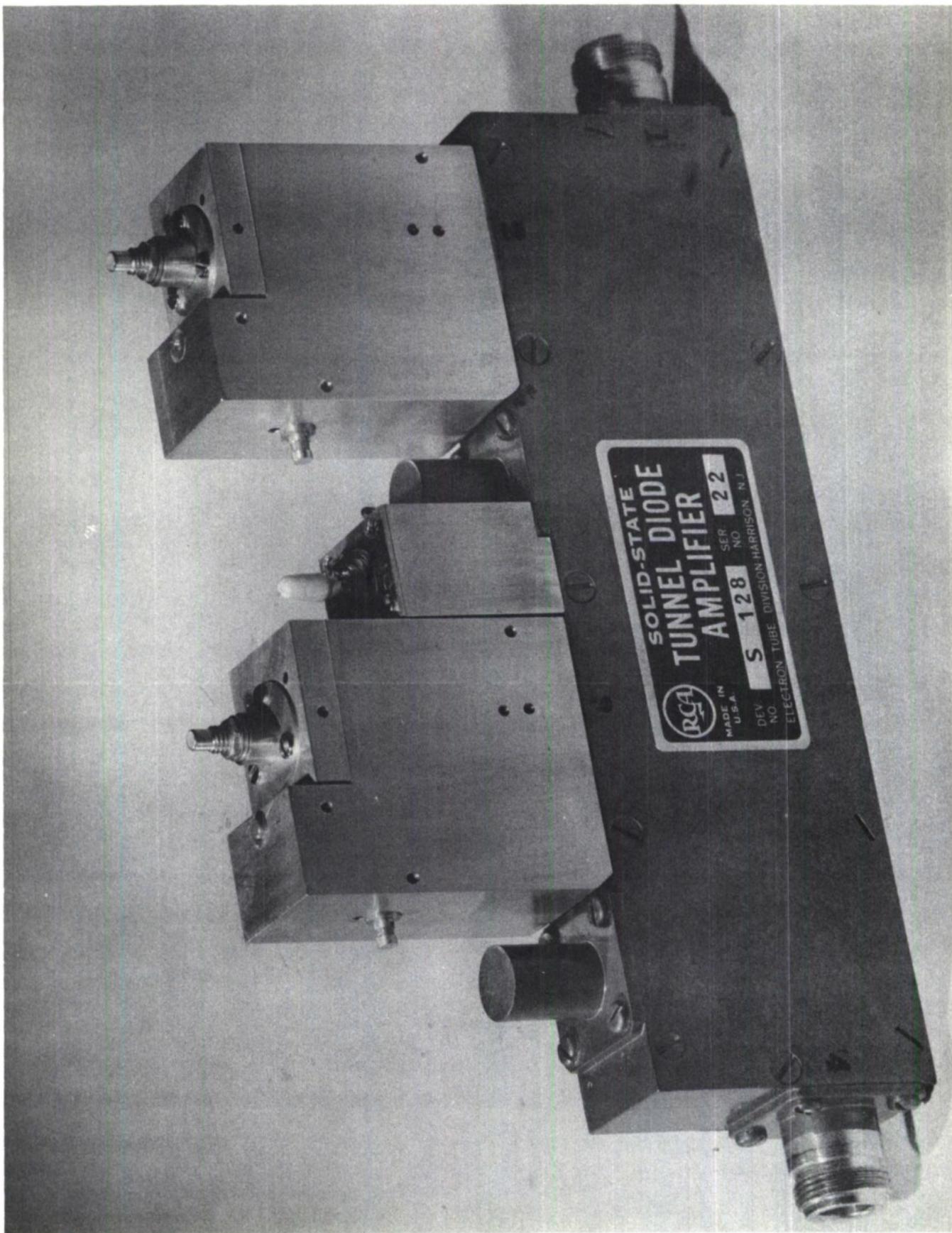
FIG. 16 PHOTOGRAPH OF S128 TUNNEL DIODE AMPLIFIER
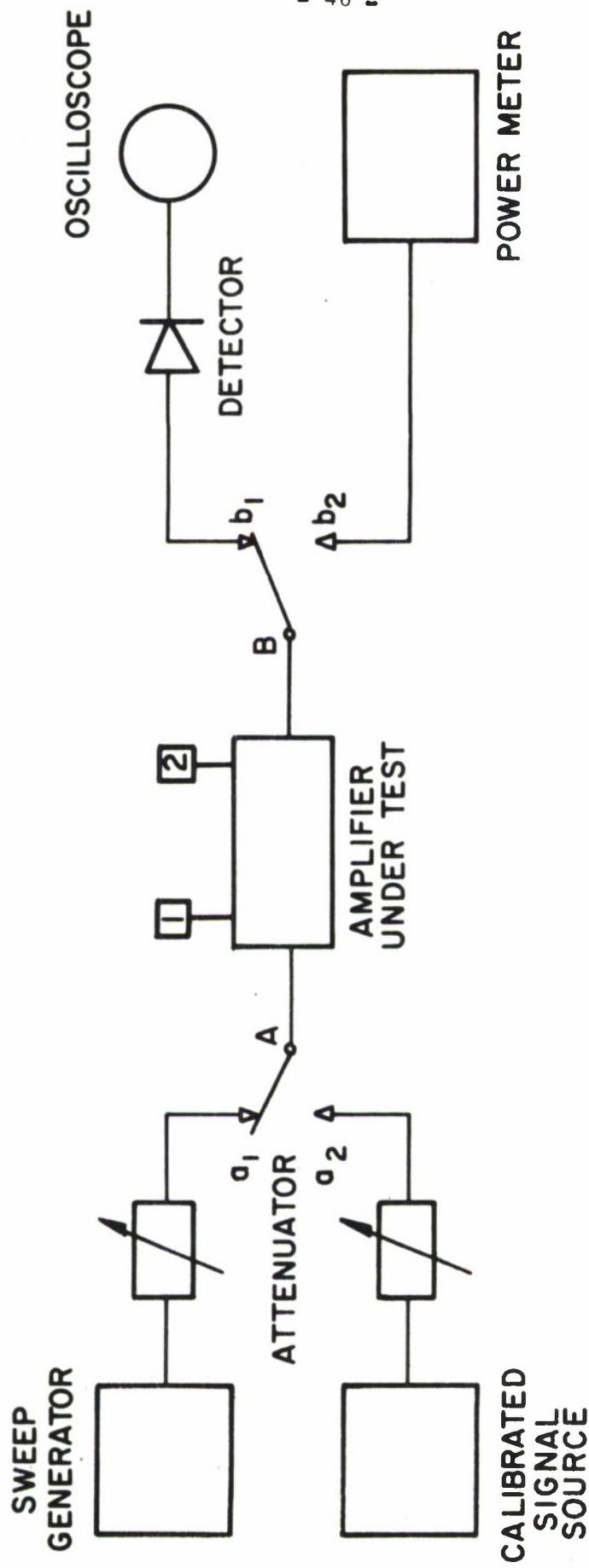
FIG. 17 AMPLITUDE TEST SET UP
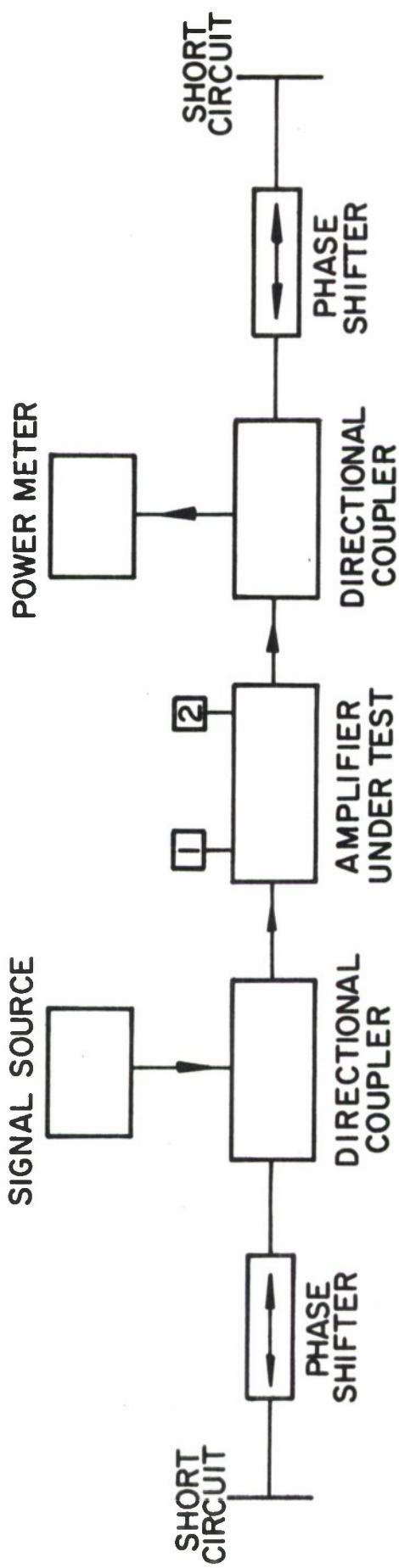
FIG. 18   INSERTION   PHASE   TEST   SET   UP
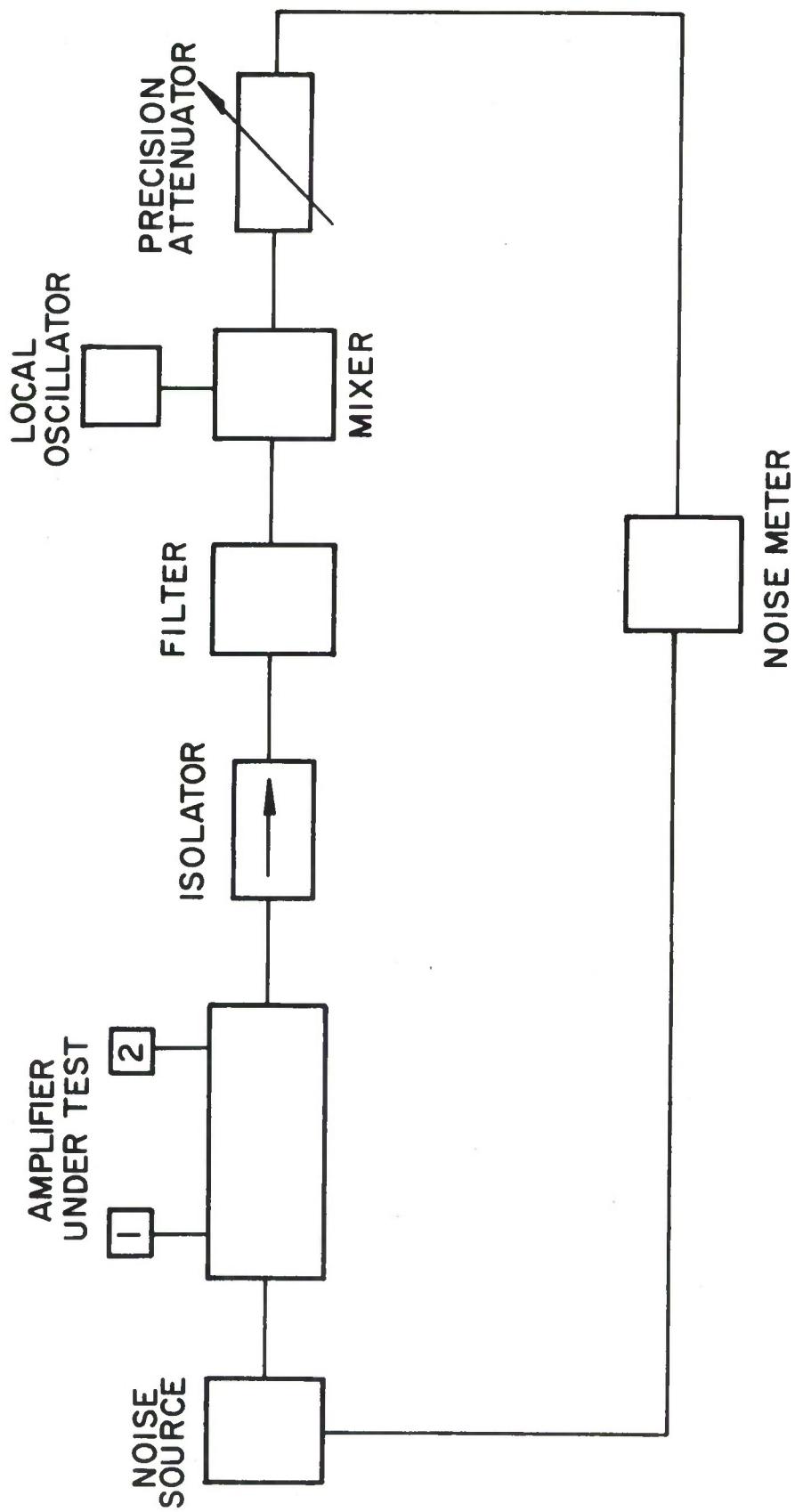
FIG. 19 NOISE FIGURE TEST — SET UP
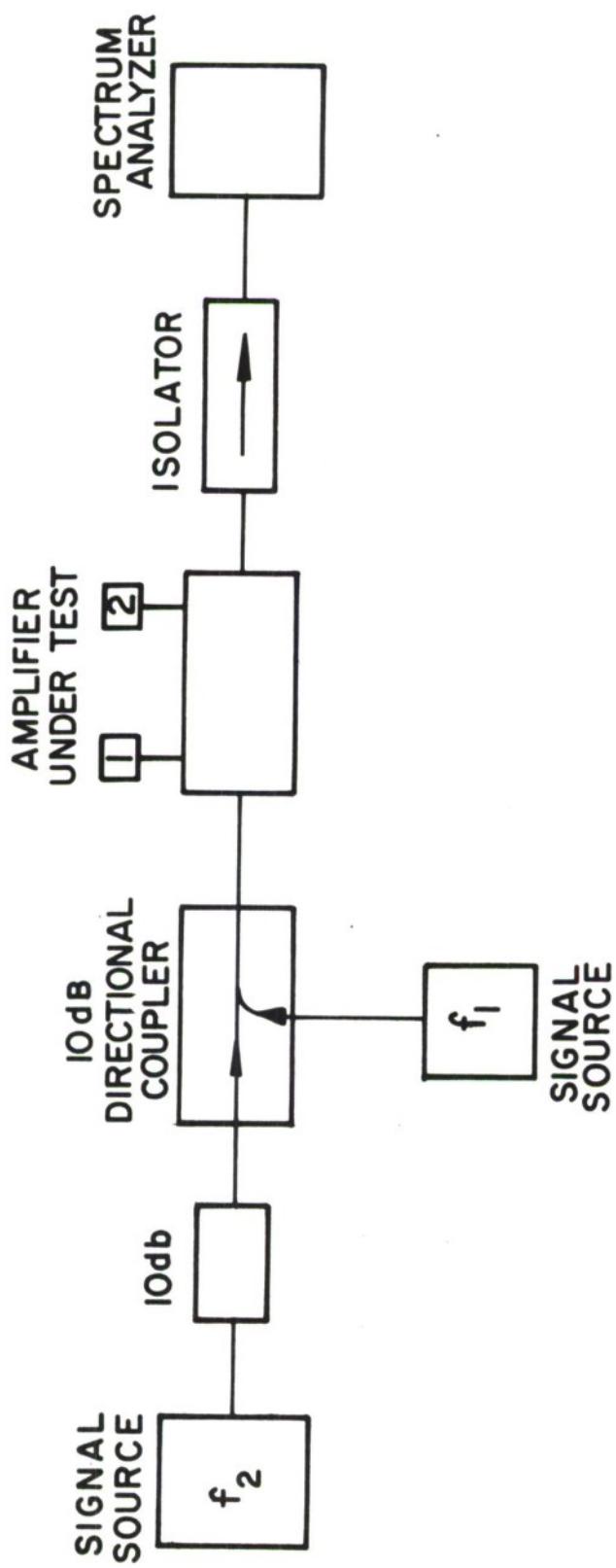
FIG. 20 TEST SET UP FOR INTERMODULATION CROSS PRODUCTS
POWER OUTPUT
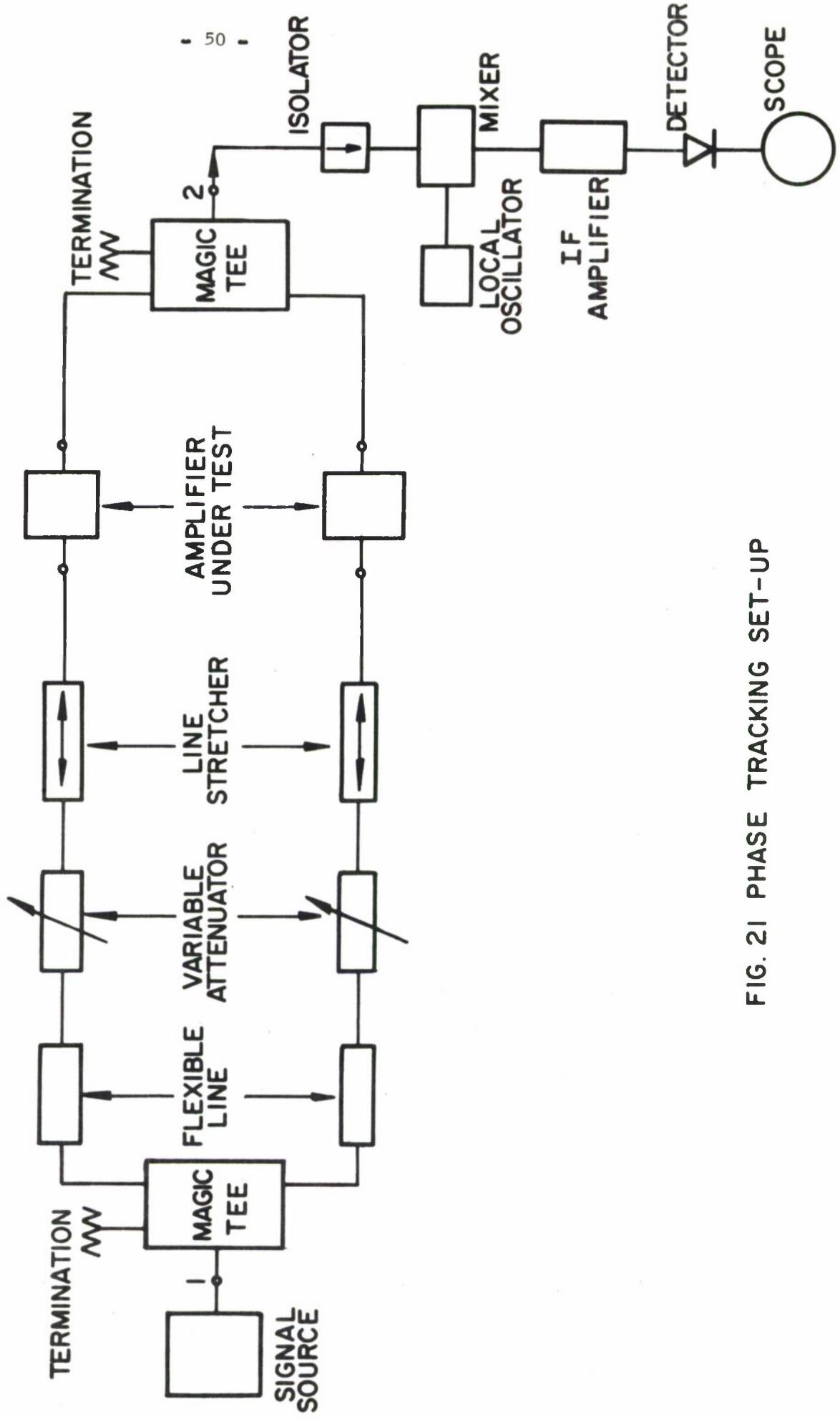
FIG. 21 PHASE TRACKING SET-UP

S128— 21

S128 — 22

S128-23

$P_{in} = -40\,dBm$
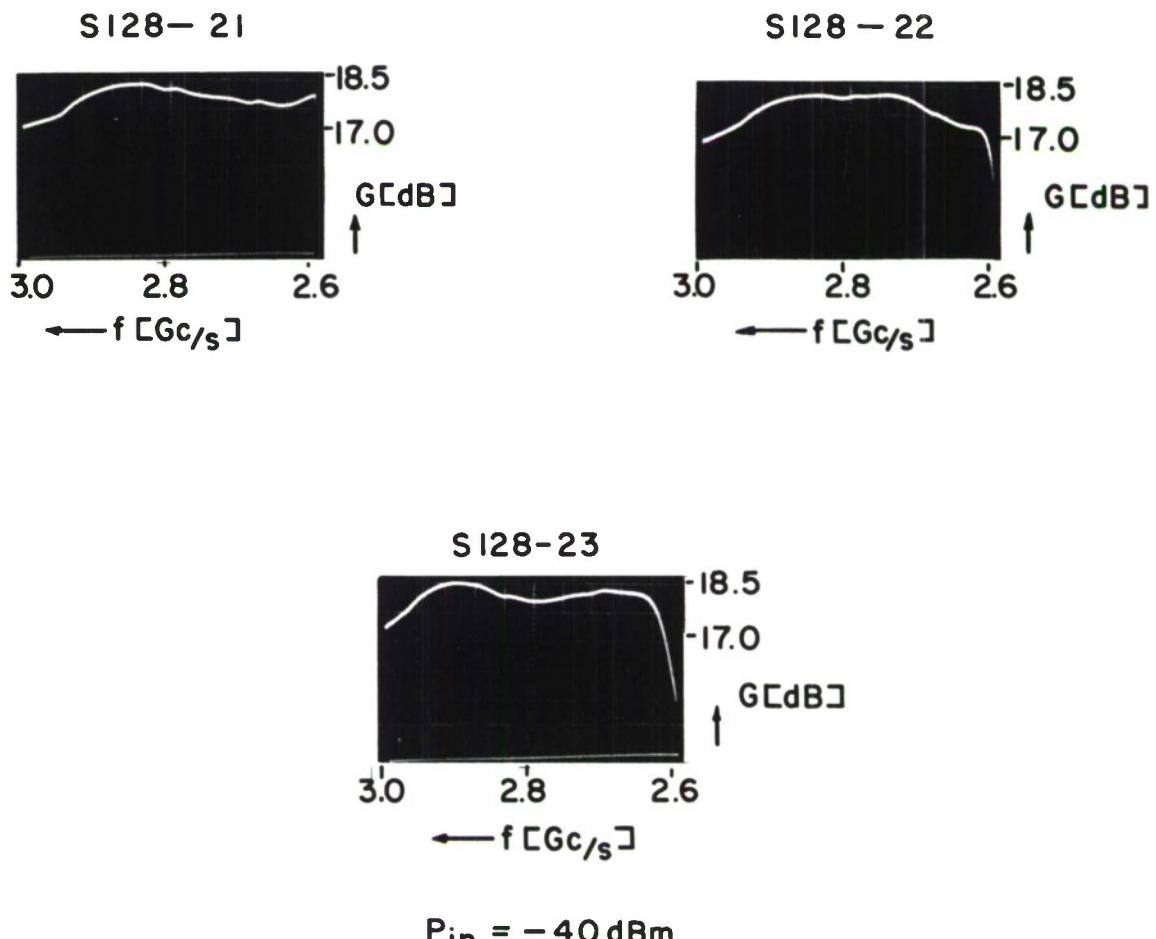
FIG. 22 SWEPT FREQUENCY RESPONSE OF THREE
S128 AMPLIFIERS
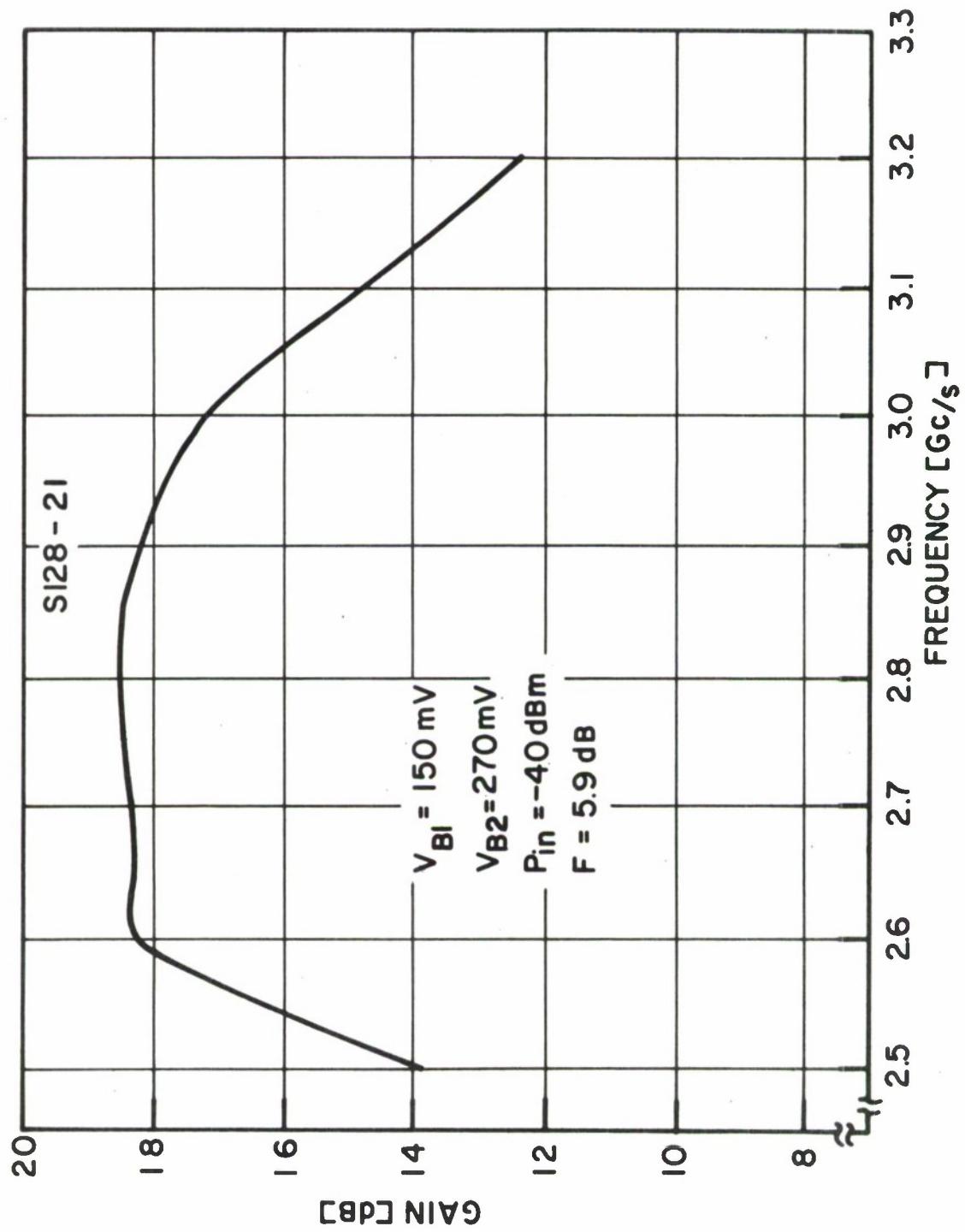
FIG. 23  GAIN vs. FREQUENCY
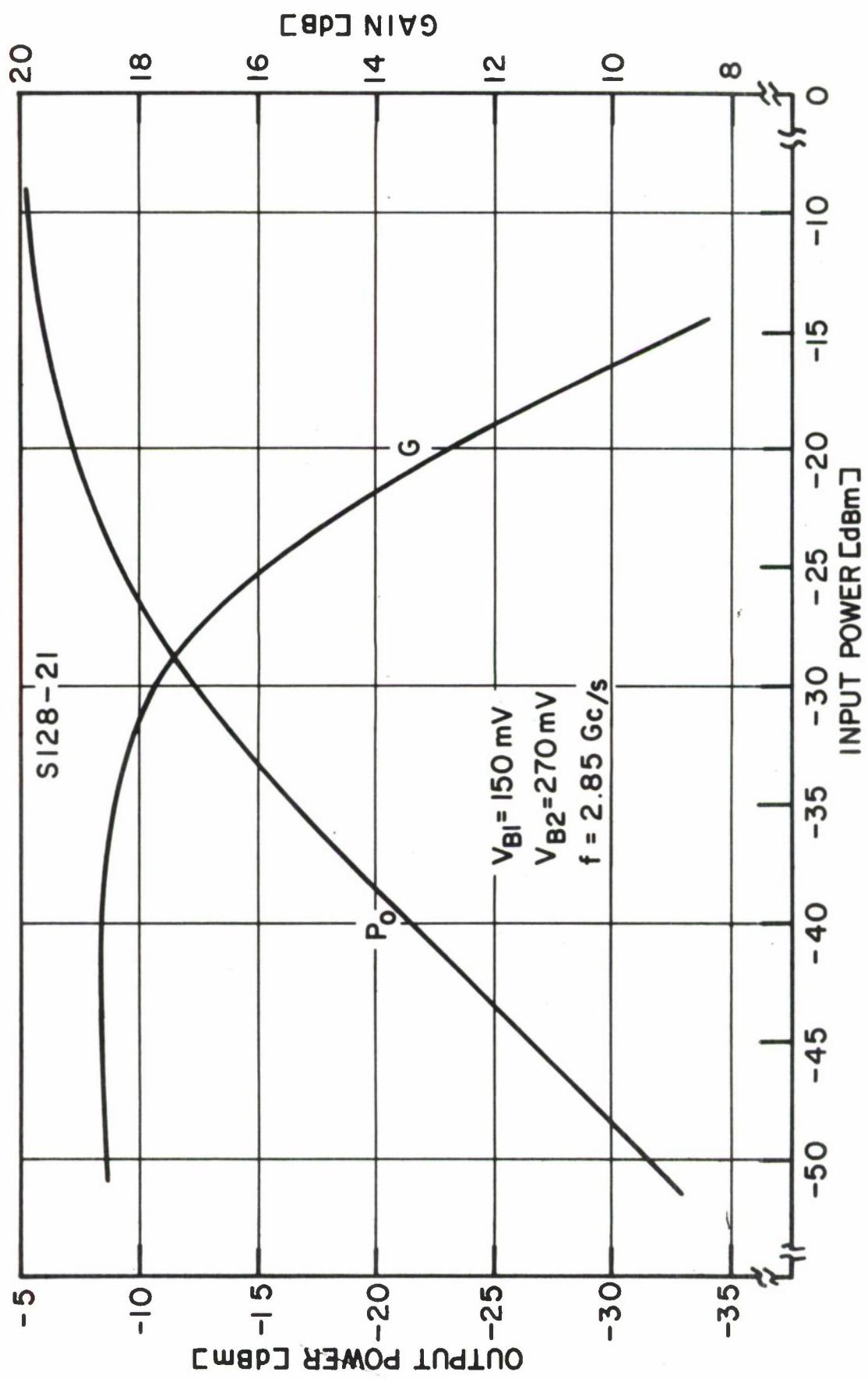
FIG. 24 SATURATION CHARACTERISTIC
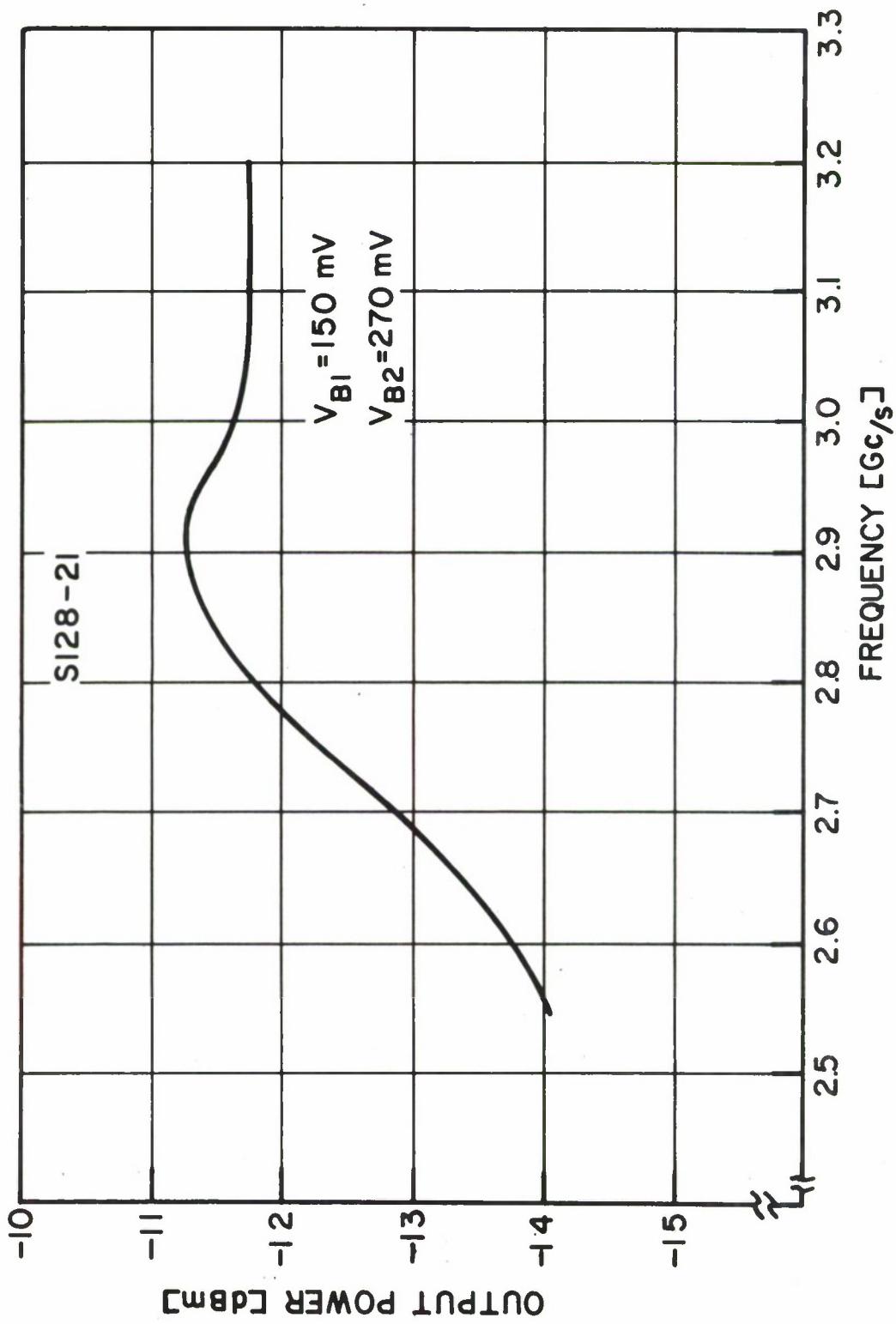
FIG. 25 OUTPUT POWER AT 1dB GAIN COMPRESSION vs.
FREQUENCY
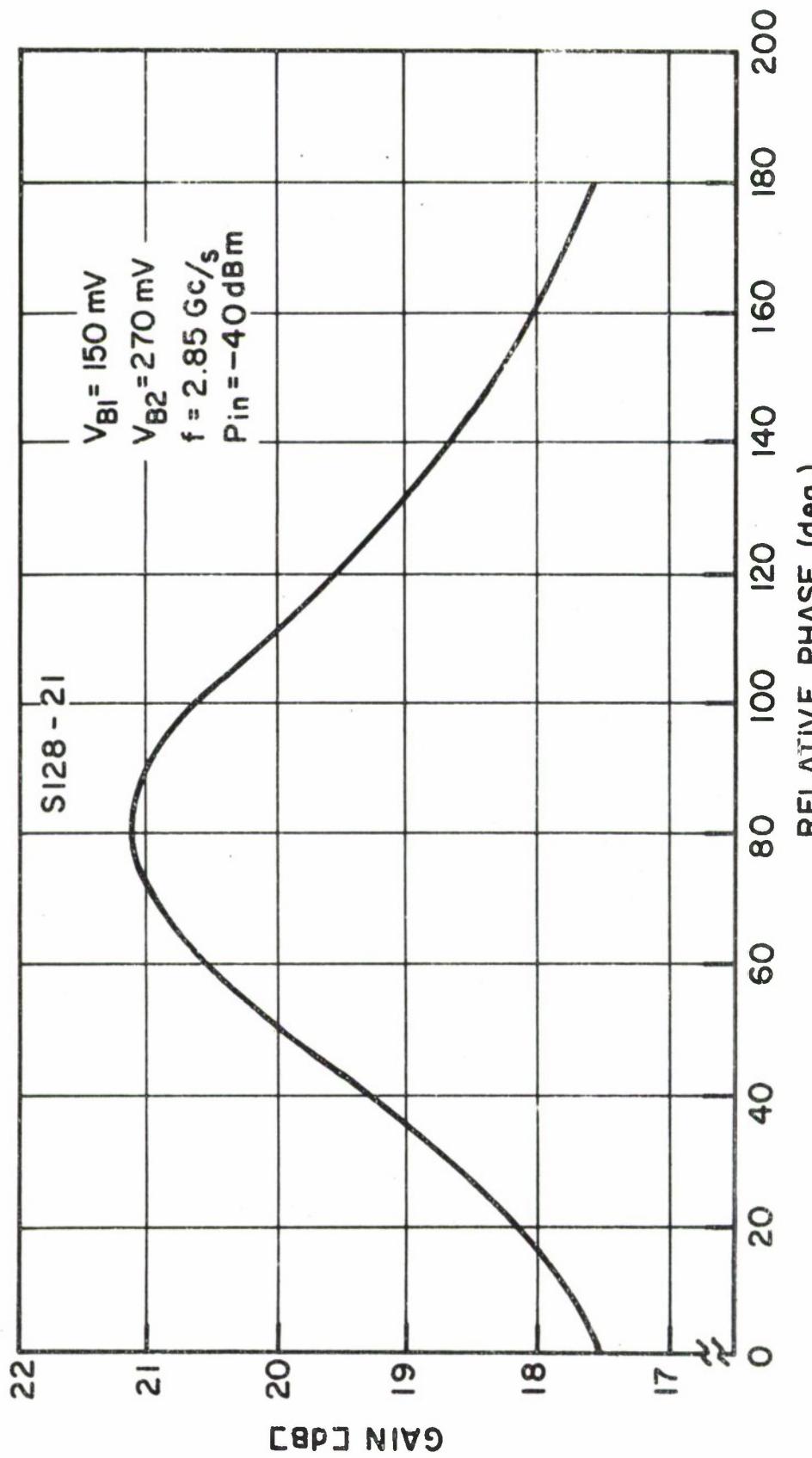
FIG. 26 GAIN vs. INSERTION PHASE
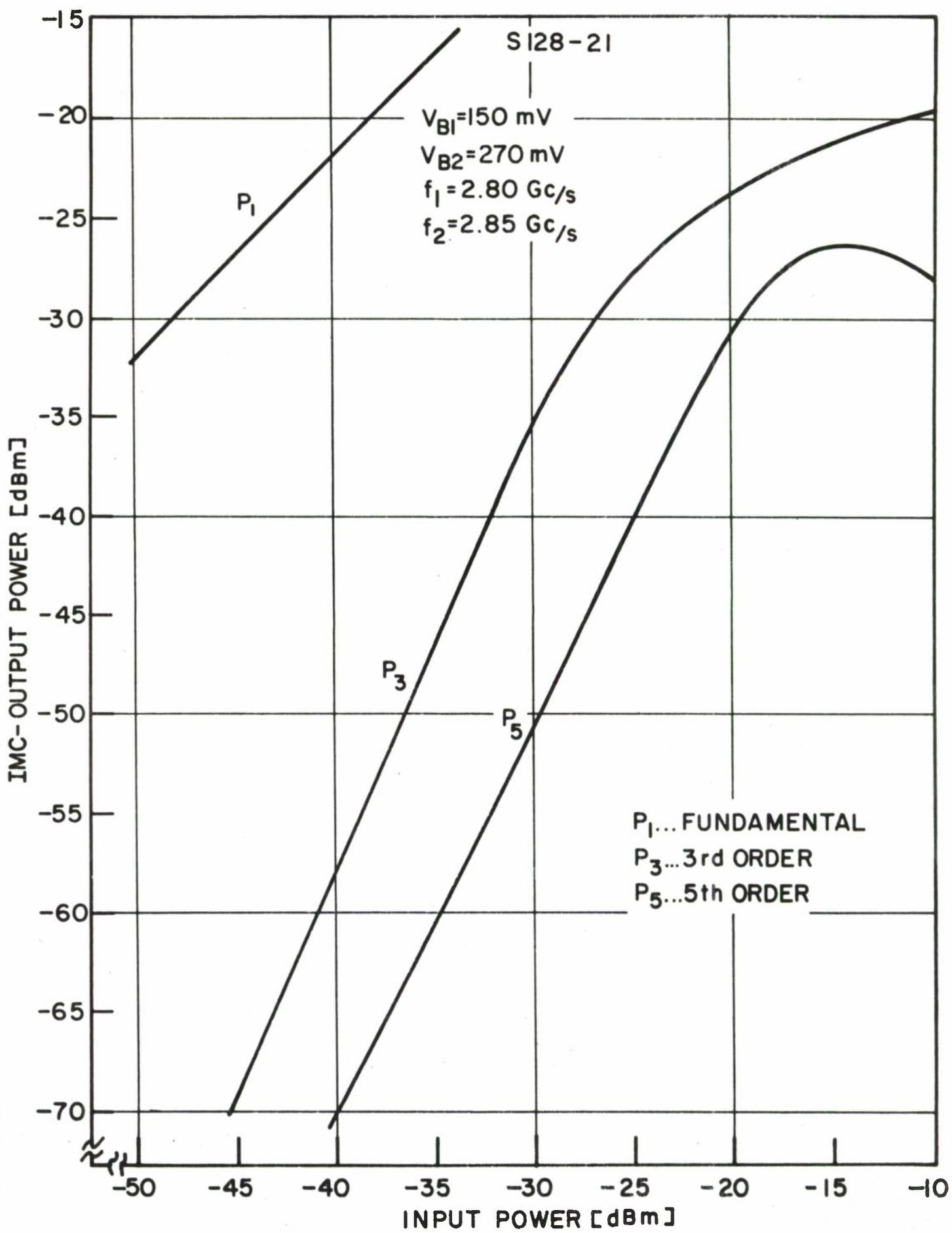
FIG. 27 IMC OUTPUT POWER vs. INPUT POWER
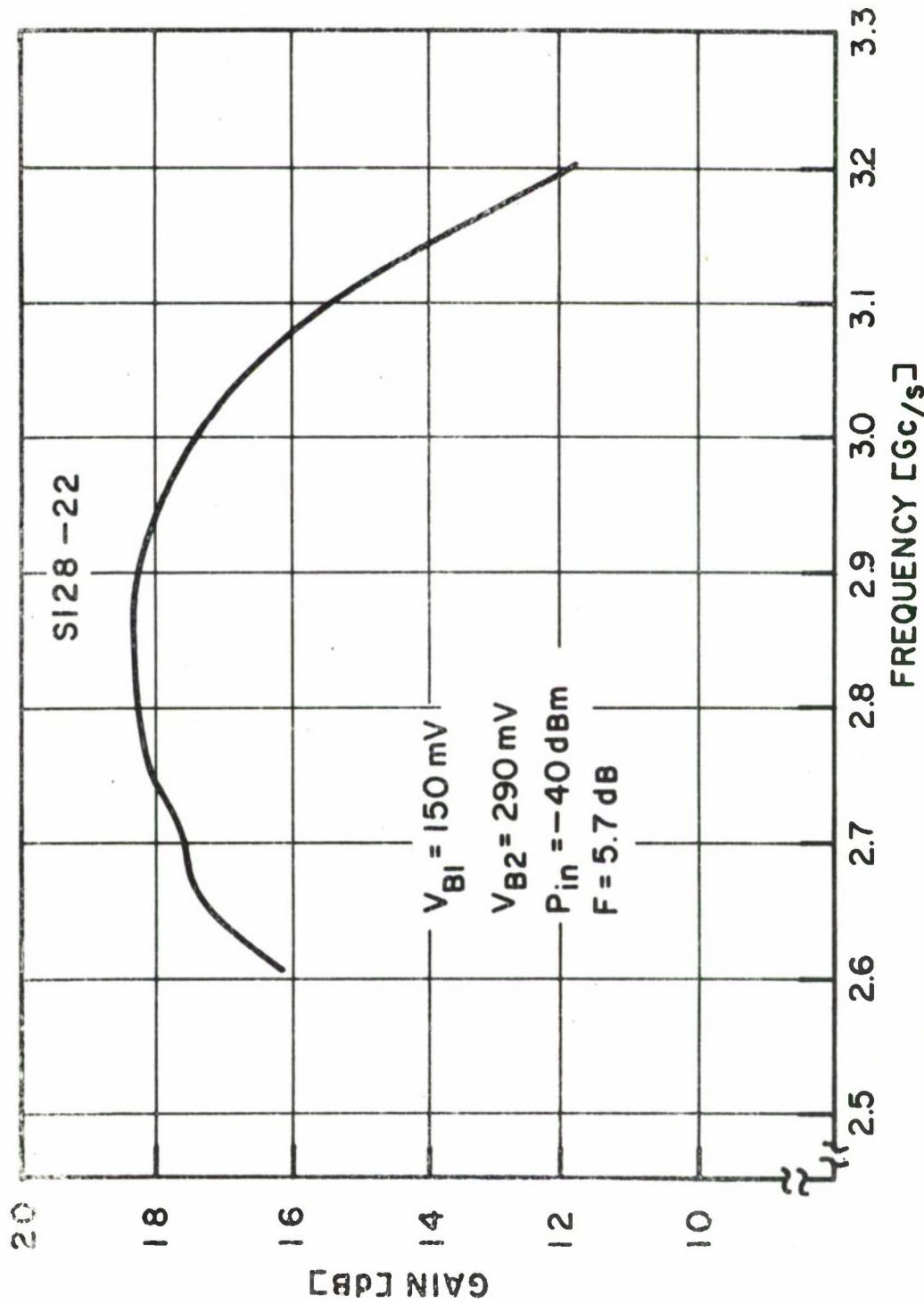
FIG. 28 GAIN vs. FREQUENCY
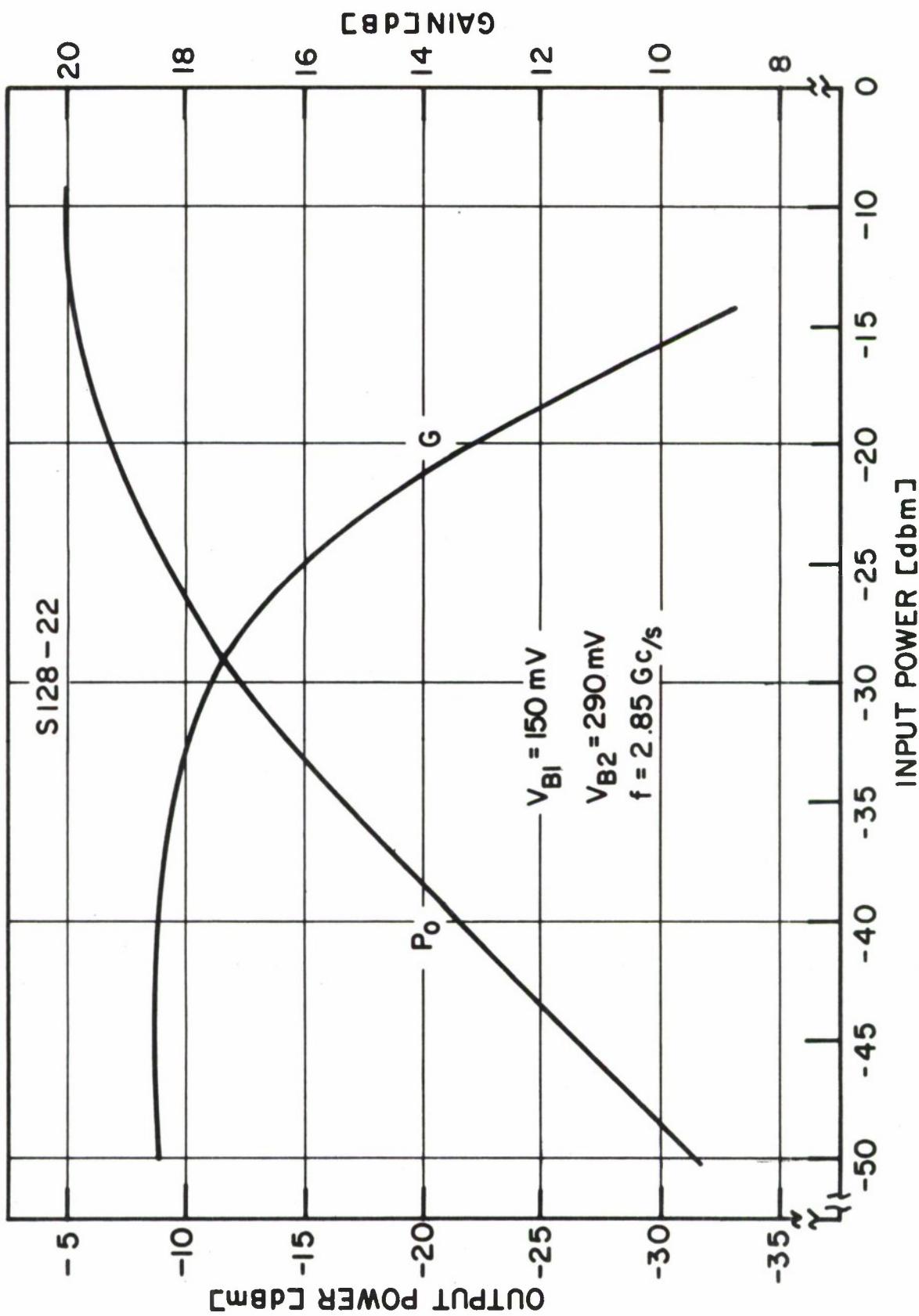
FIG. 29 SATURATION CHARACTERISTIC
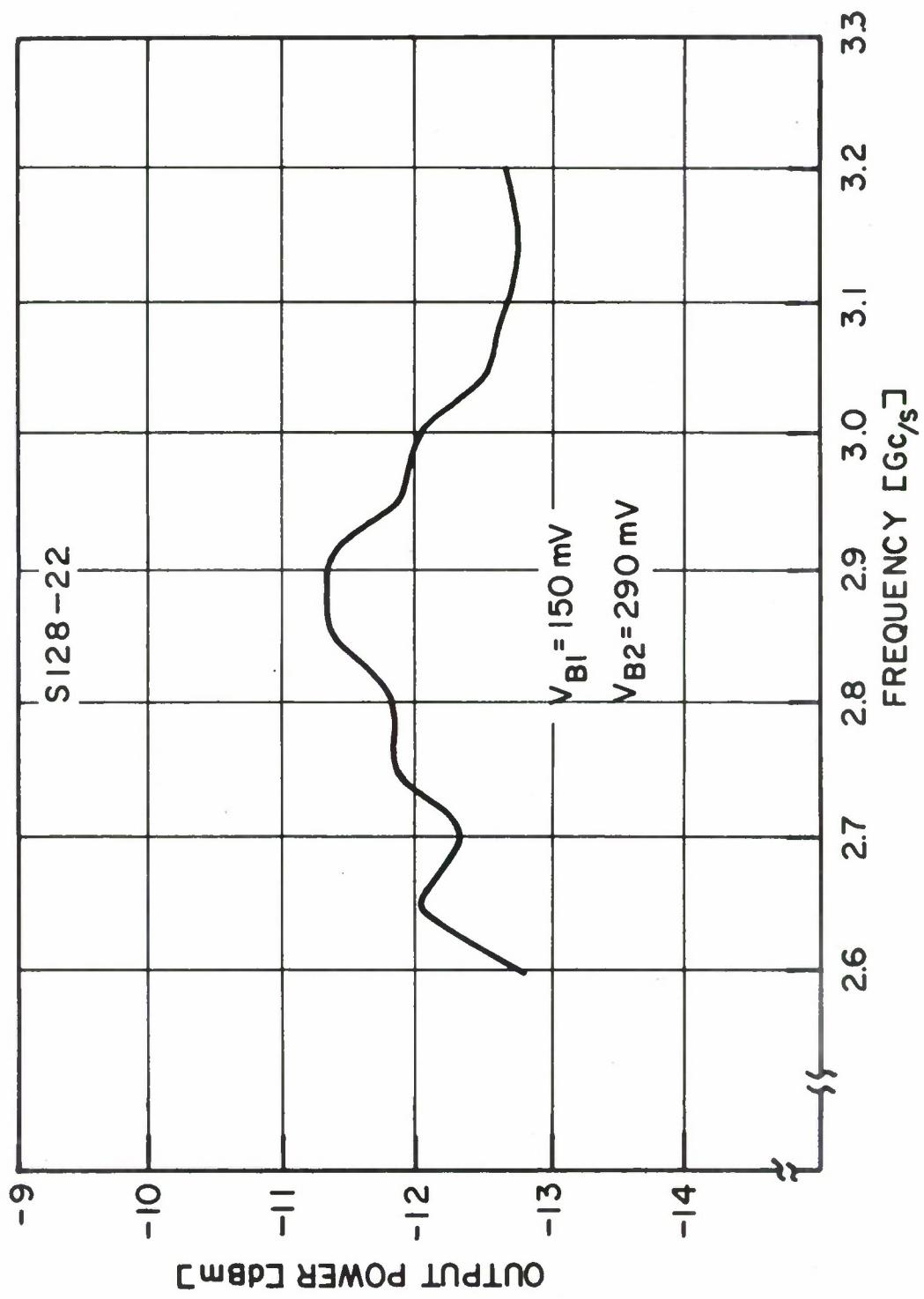
FIG. 30 OUTPUT POWER AT 1 dB GAIN COMPRESSION vs. FREQUENCY
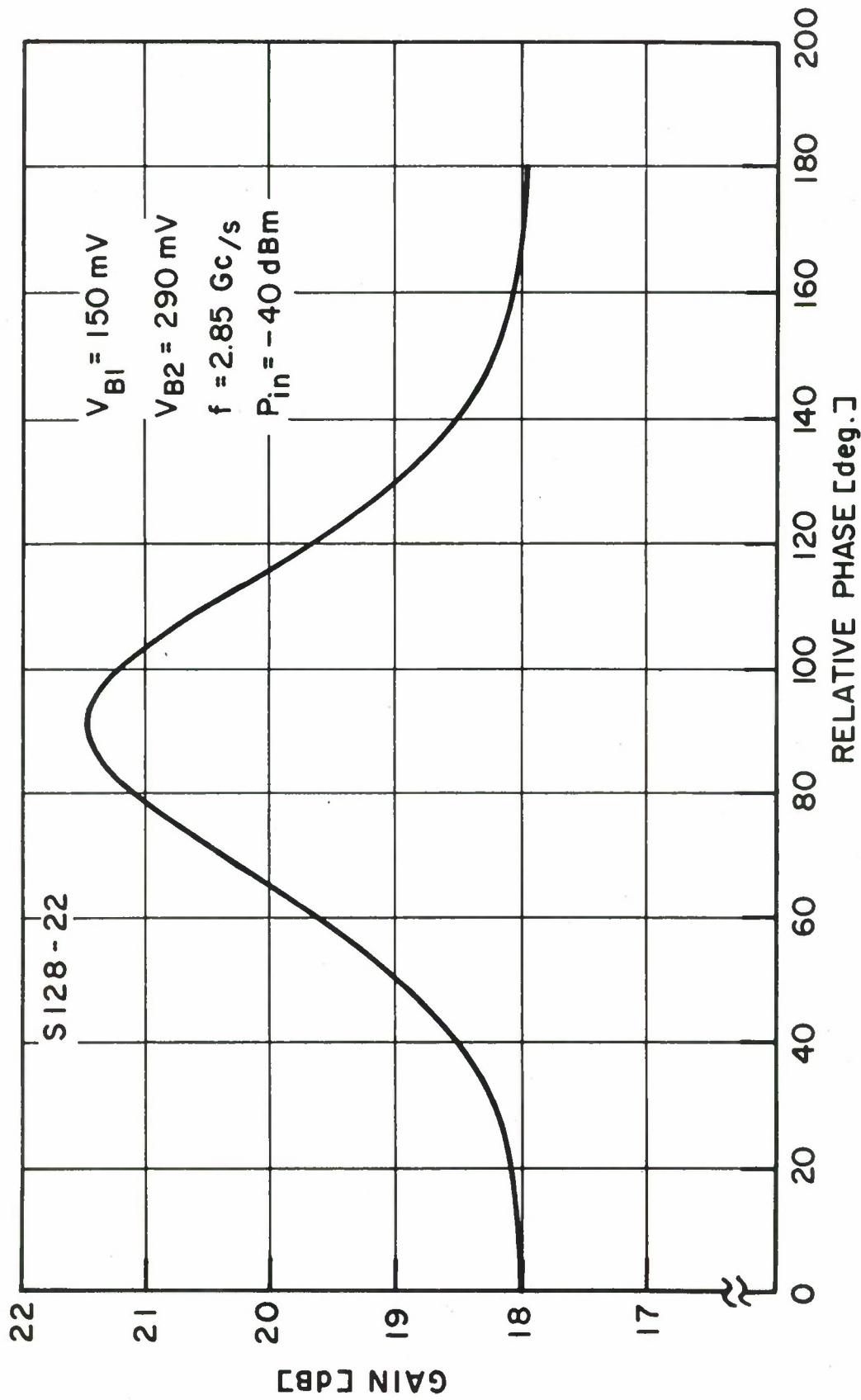
FIG. 31 GAIN vs. INSERTION PHASE
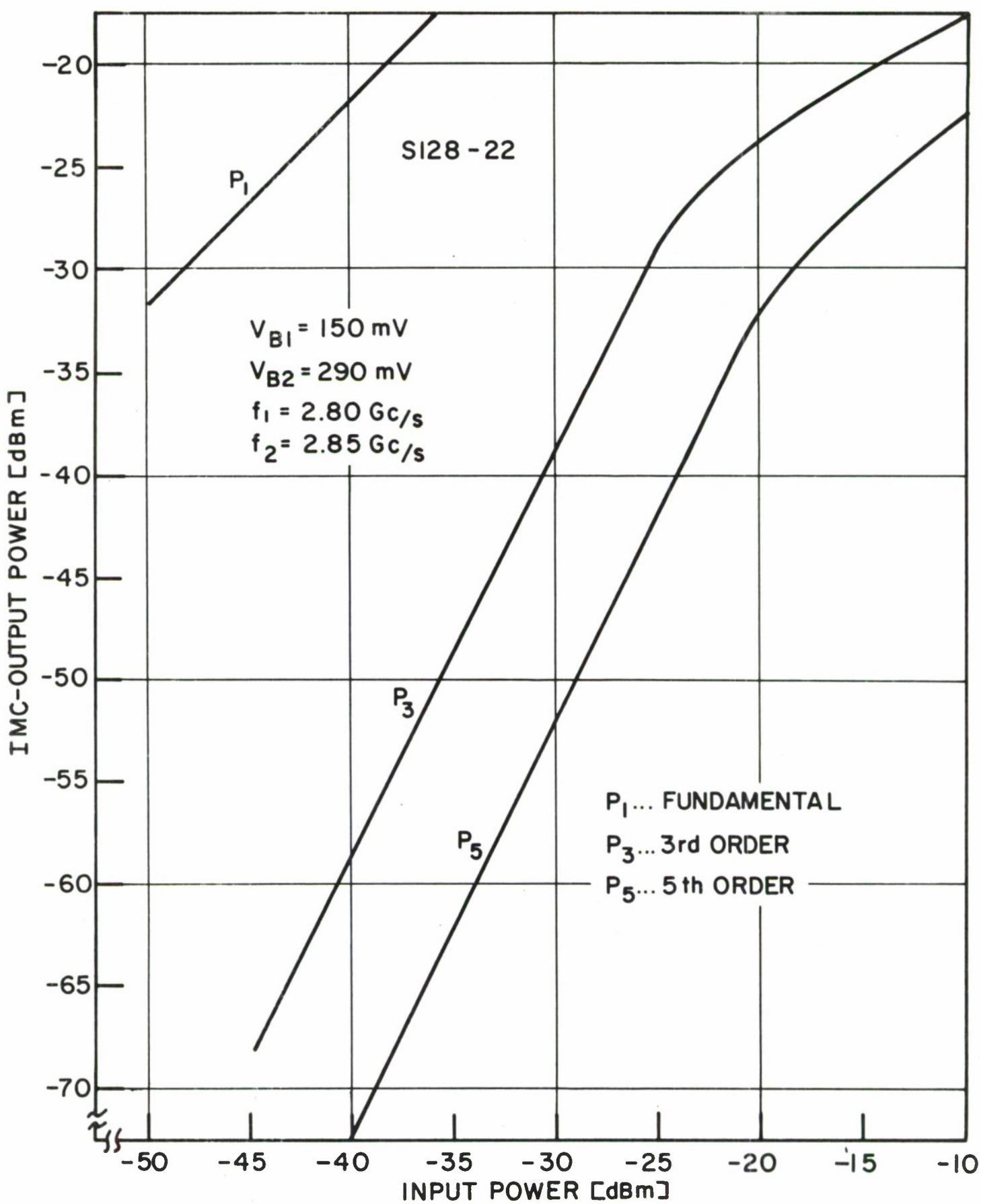
FIG. 32 IMC-OUTPUT POWER vs. INPUT POWER
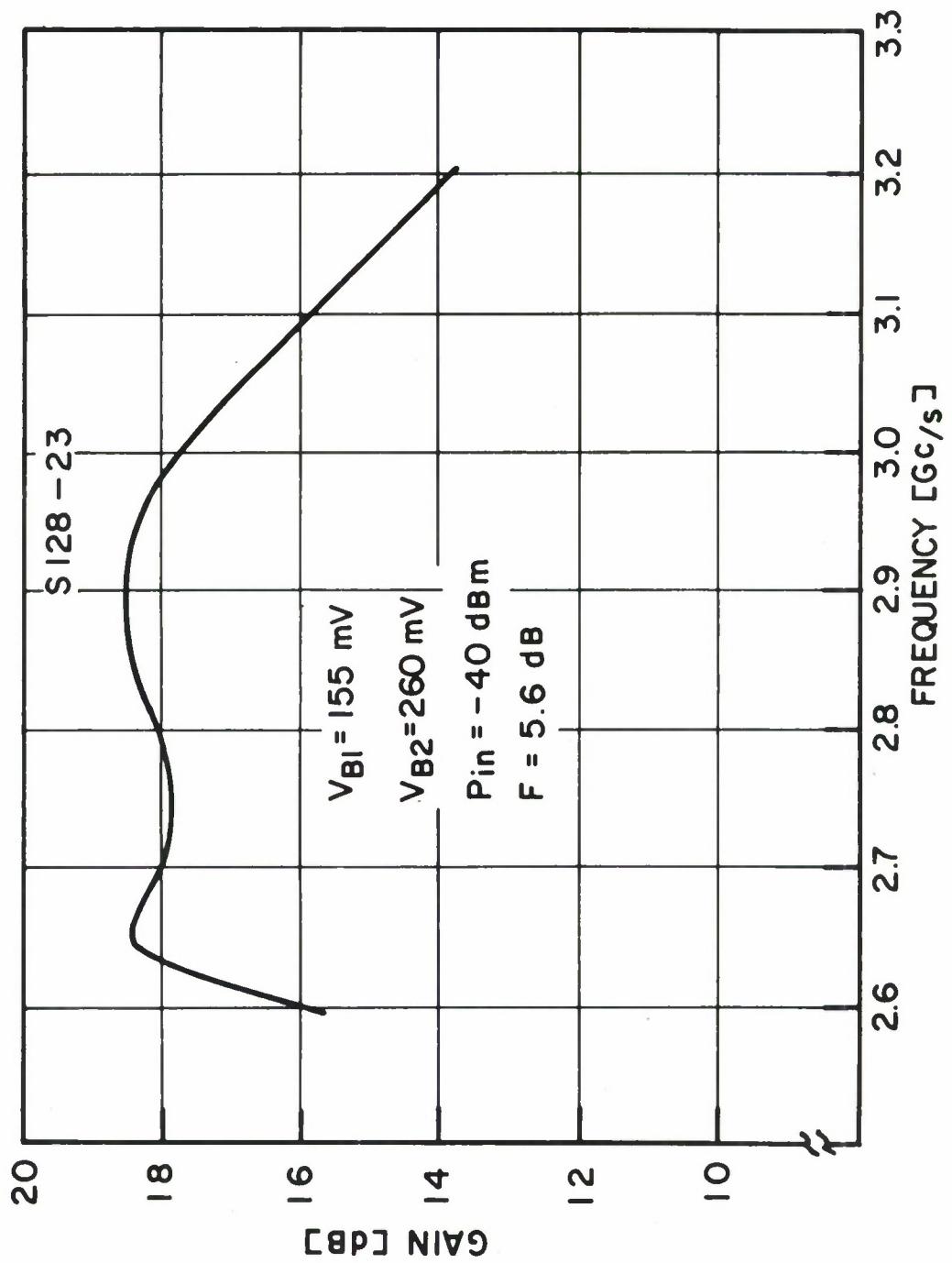
FIG. 33 GAIN vs. FREQUENCY
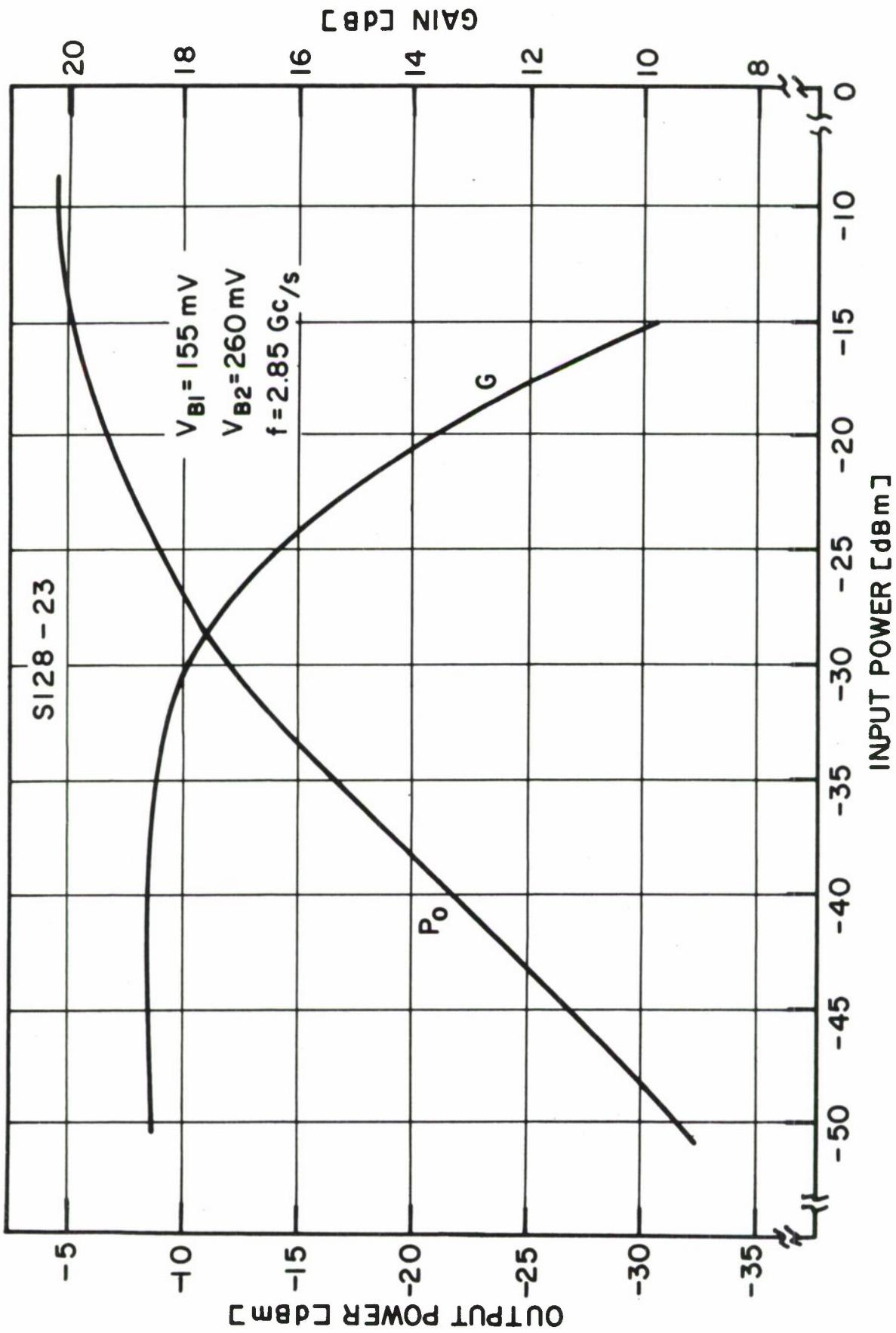
FIG. 34 SATURATION CHARACTERISTIC
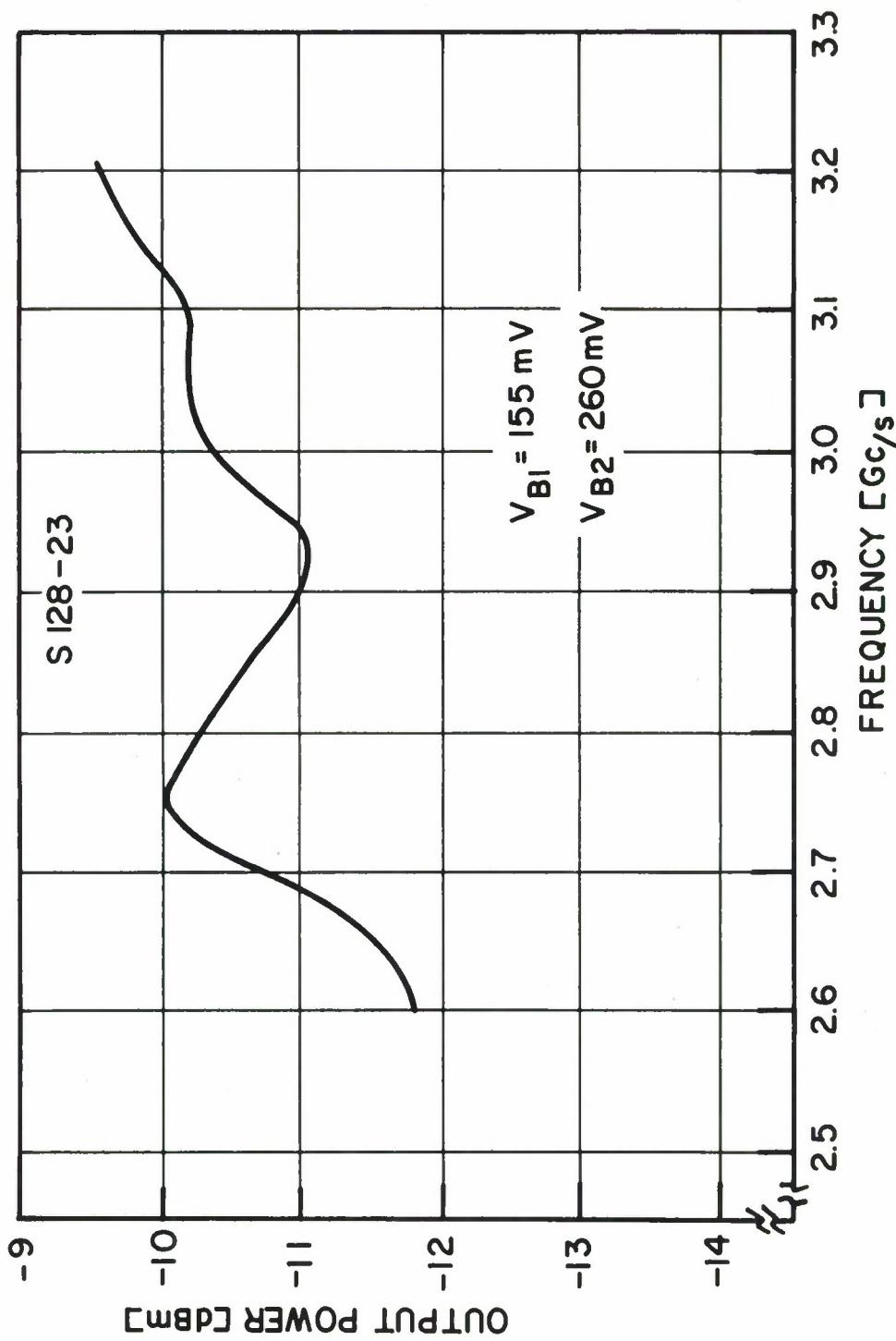
FIG. 35 OUTPUT POWER AT 1dB GAIN COMPRESSION vs. FREQUENCY
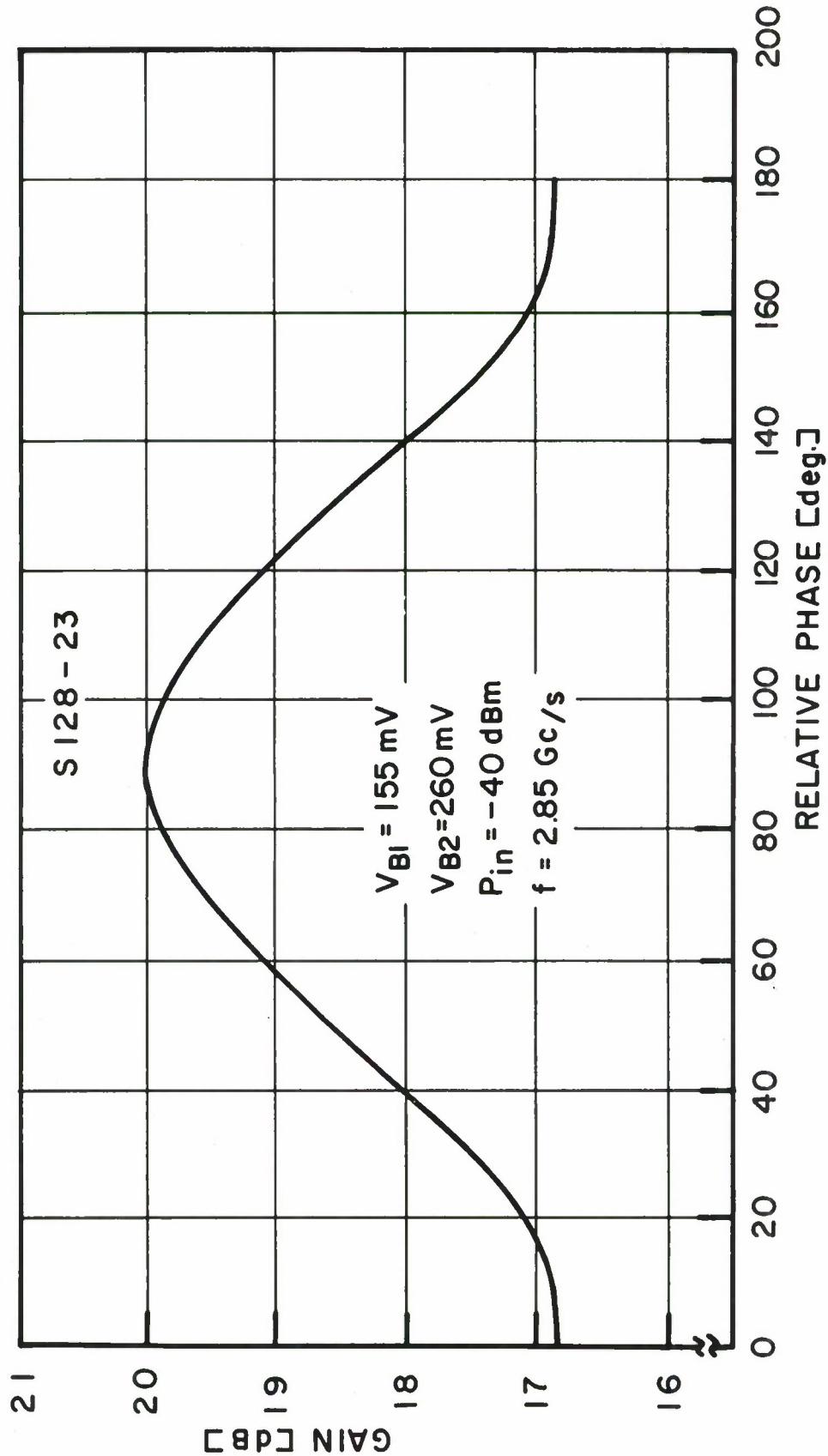
FIG. 36 GAIN vs. INSERTION PHASE
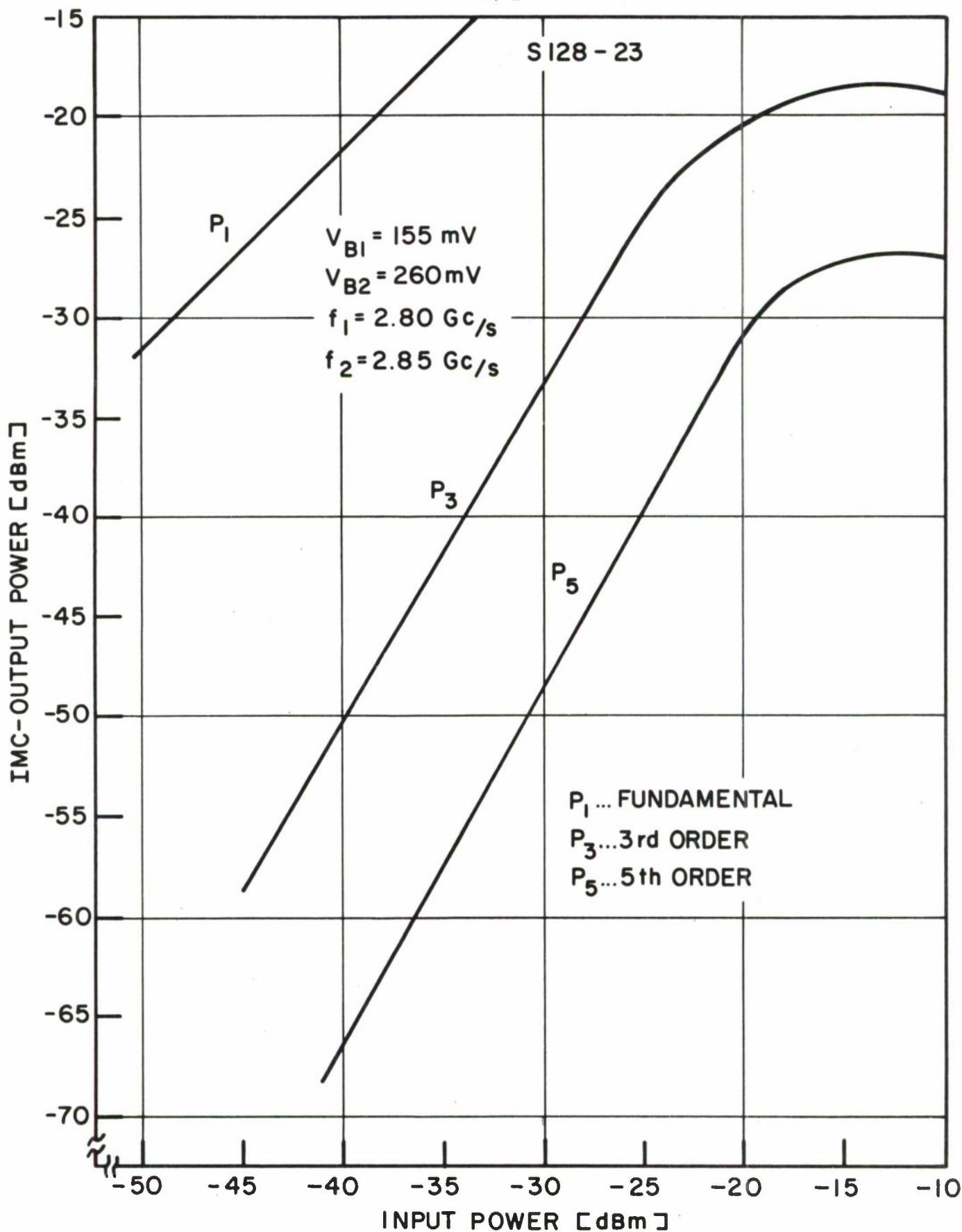
FIG. 37 IMC−OUTPUT POWER vs. INPUT POWER
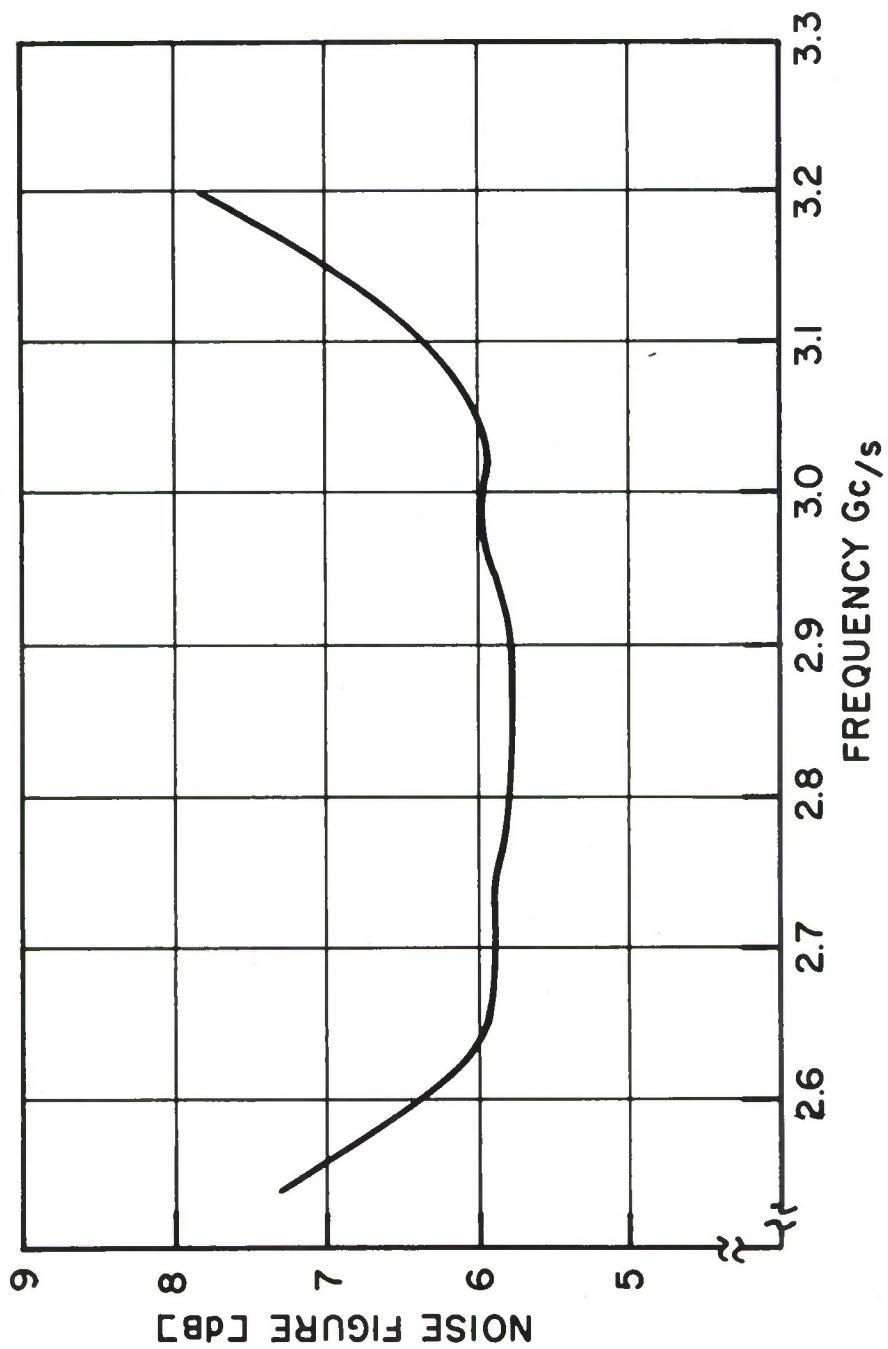
FIG. 38 TYPICAL SI28 NOISE FIGURE vs. FREQUENCY PLOT
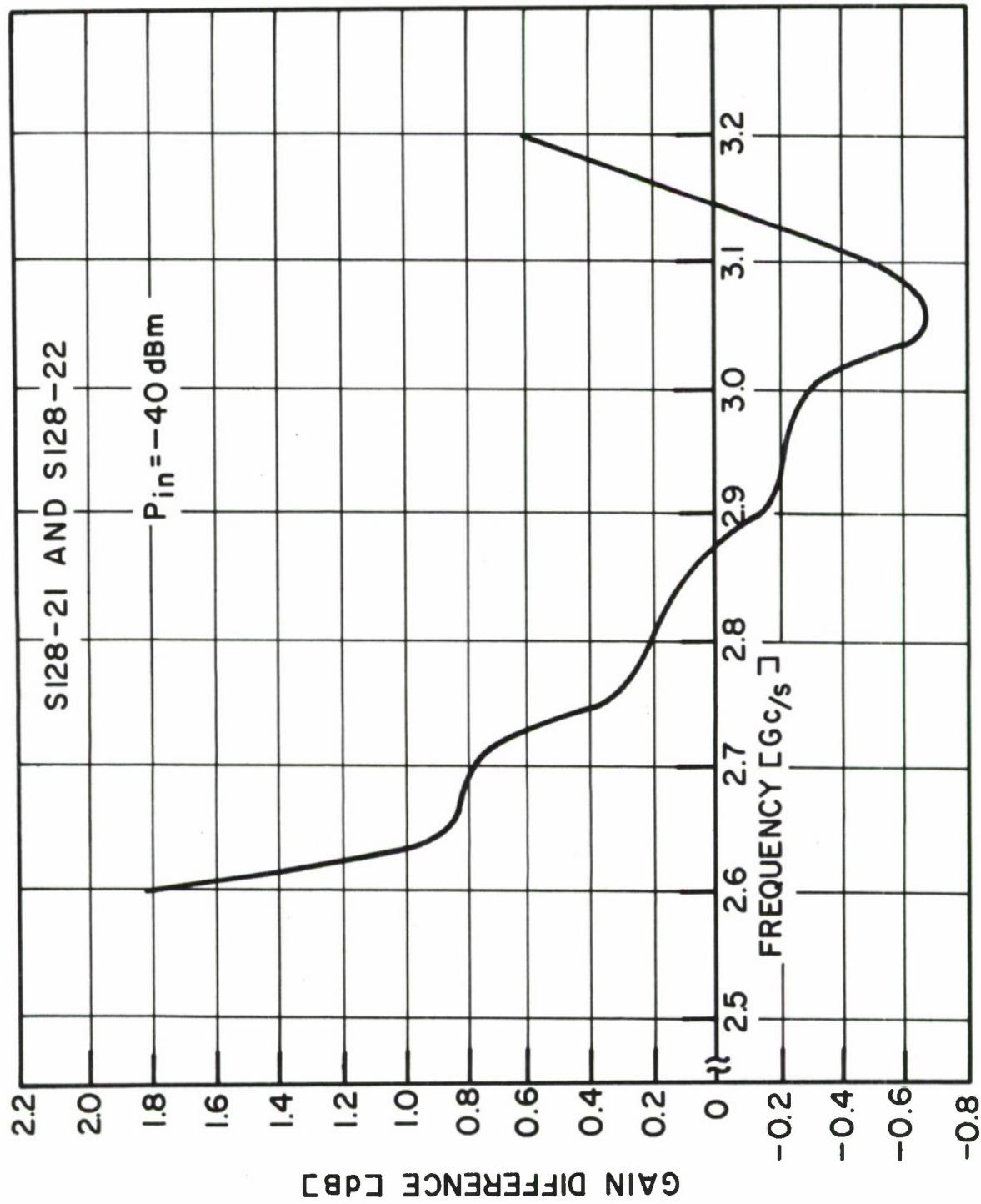
FIG. 39 AMPLITUDE TRACKING vs. FREQUENCY

FIG. 40 PHASE TRACKING vs. FREQUENCY

S128-21 AND S128-22

f=2.85 Gc/s

2.90

2.80

PHASE DIFFERENCE [deg.]
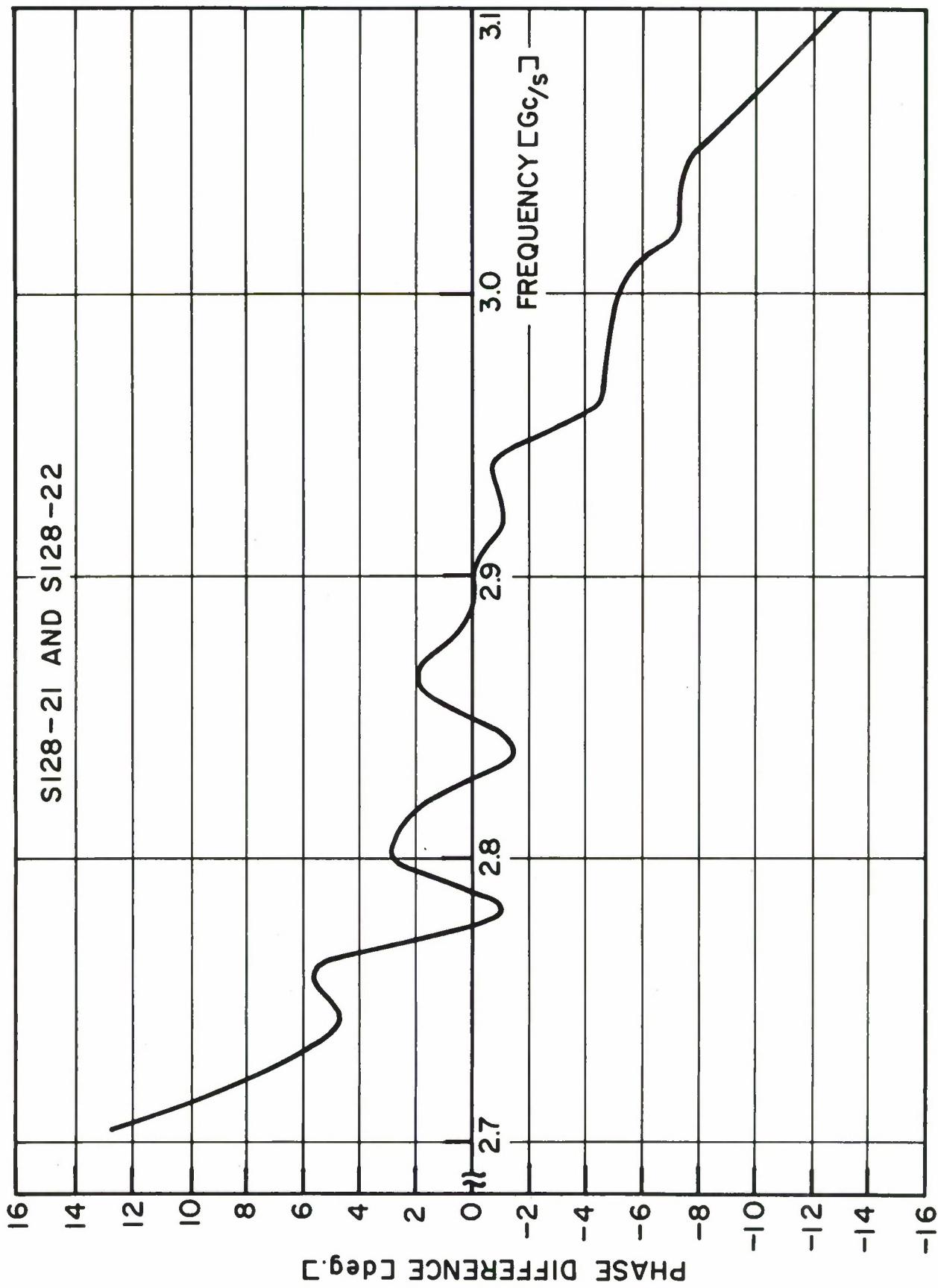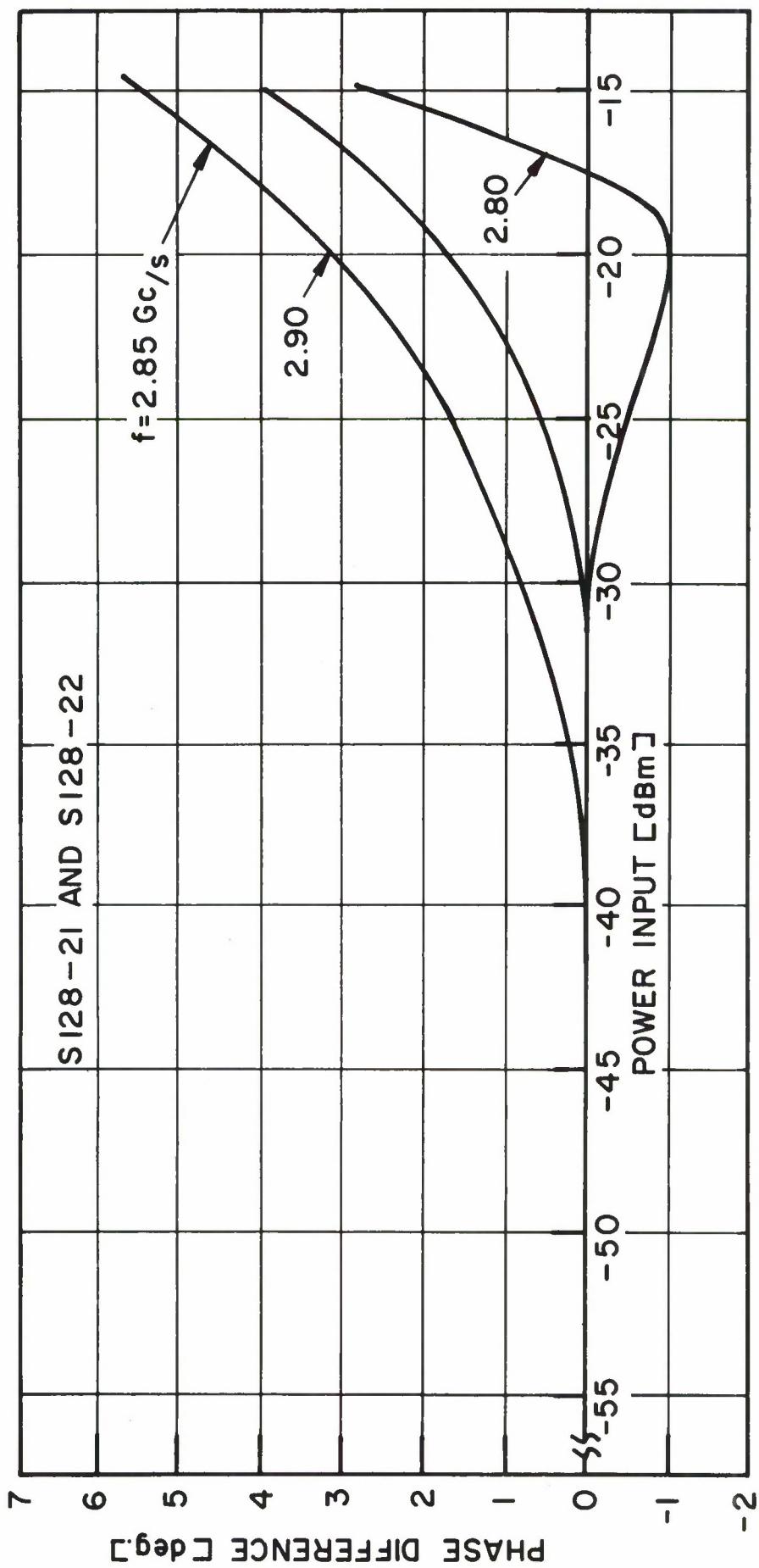
POWER INPUT [dBm]

FIG. 41 PHASE TRACKING vs. POWER INPUT
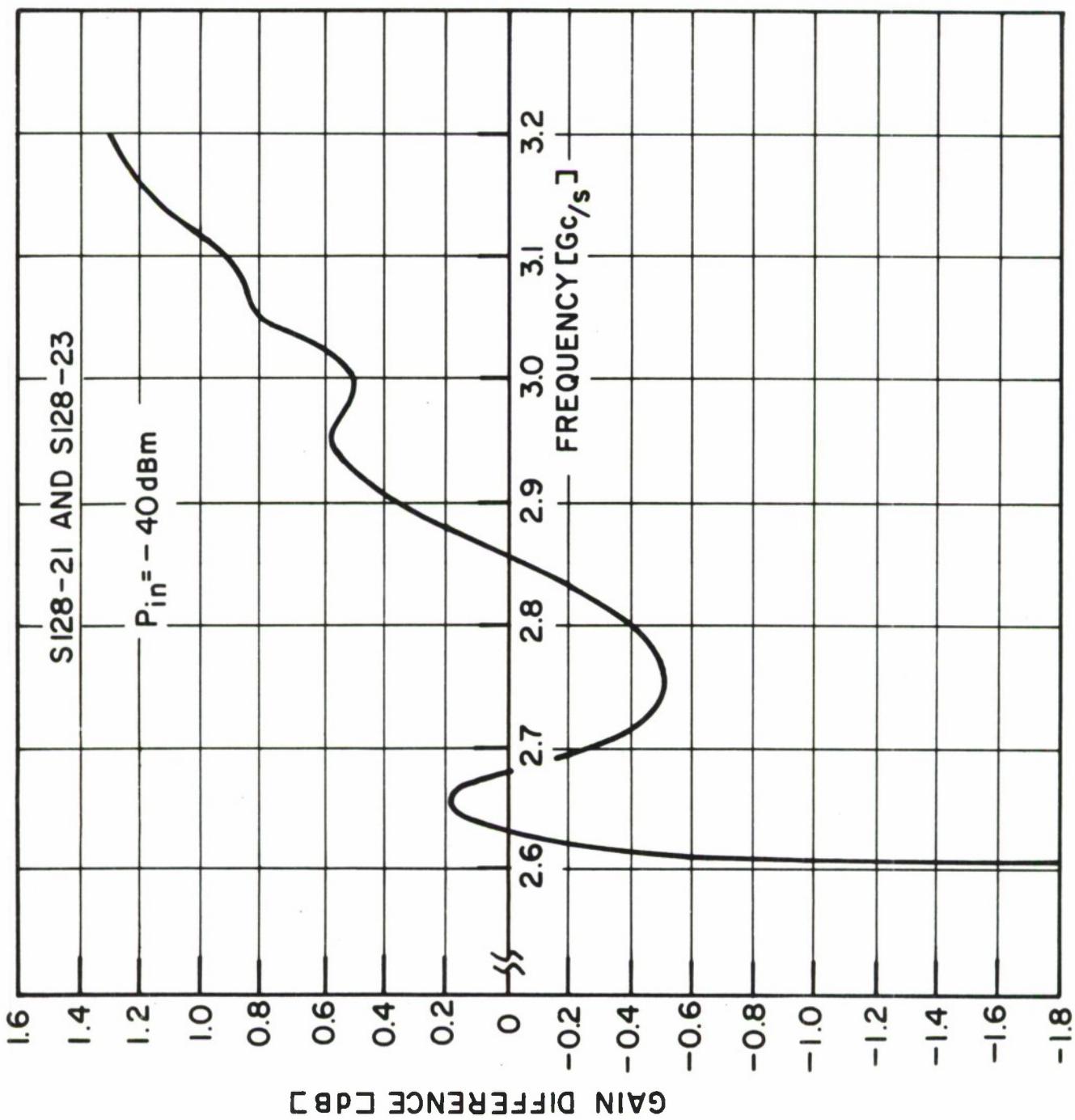
FIG. 42 AMPLITUDE TRACKING vs. FREQUENCY
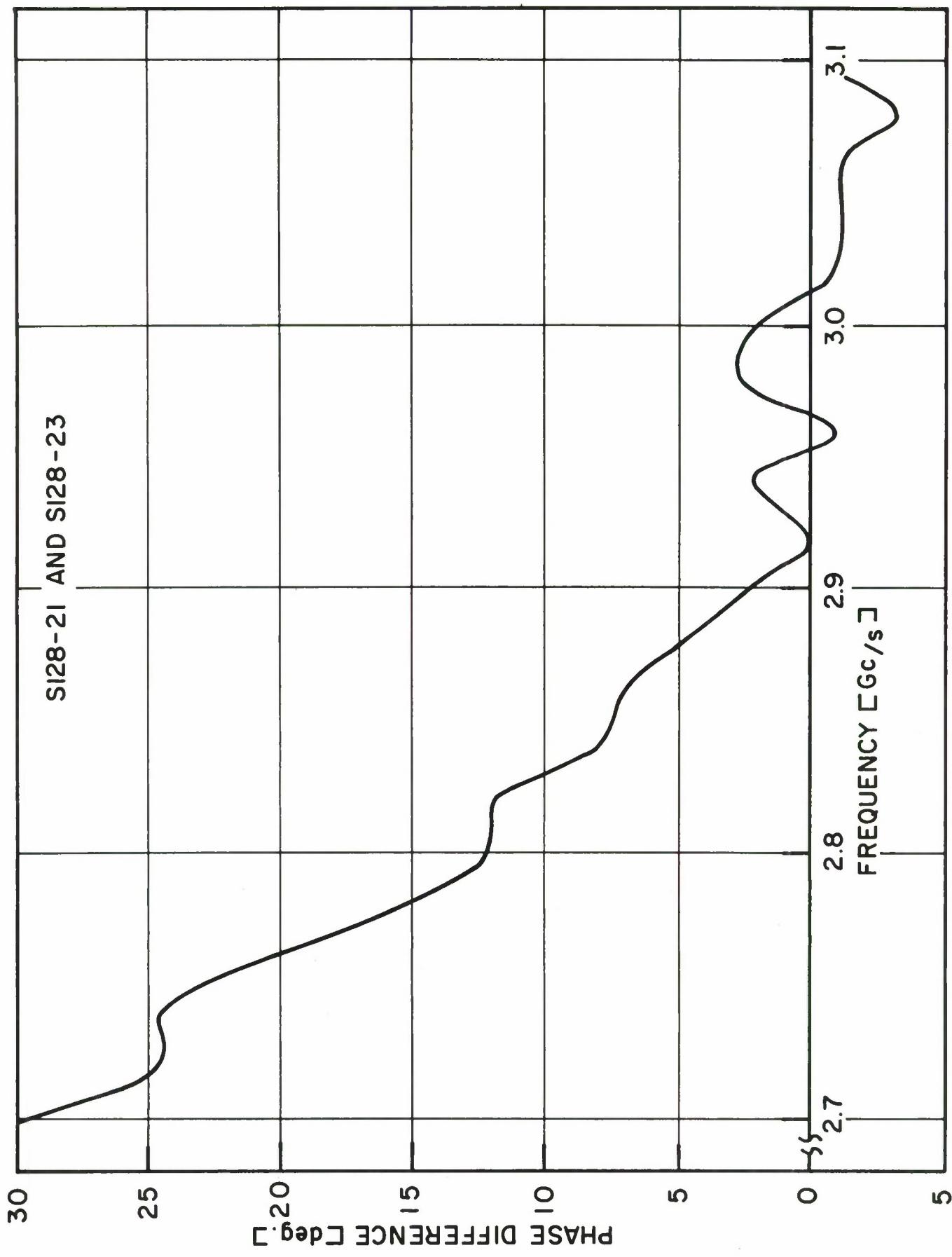
FIG. 43 PHASE TRACKING vs. FREQUENCY
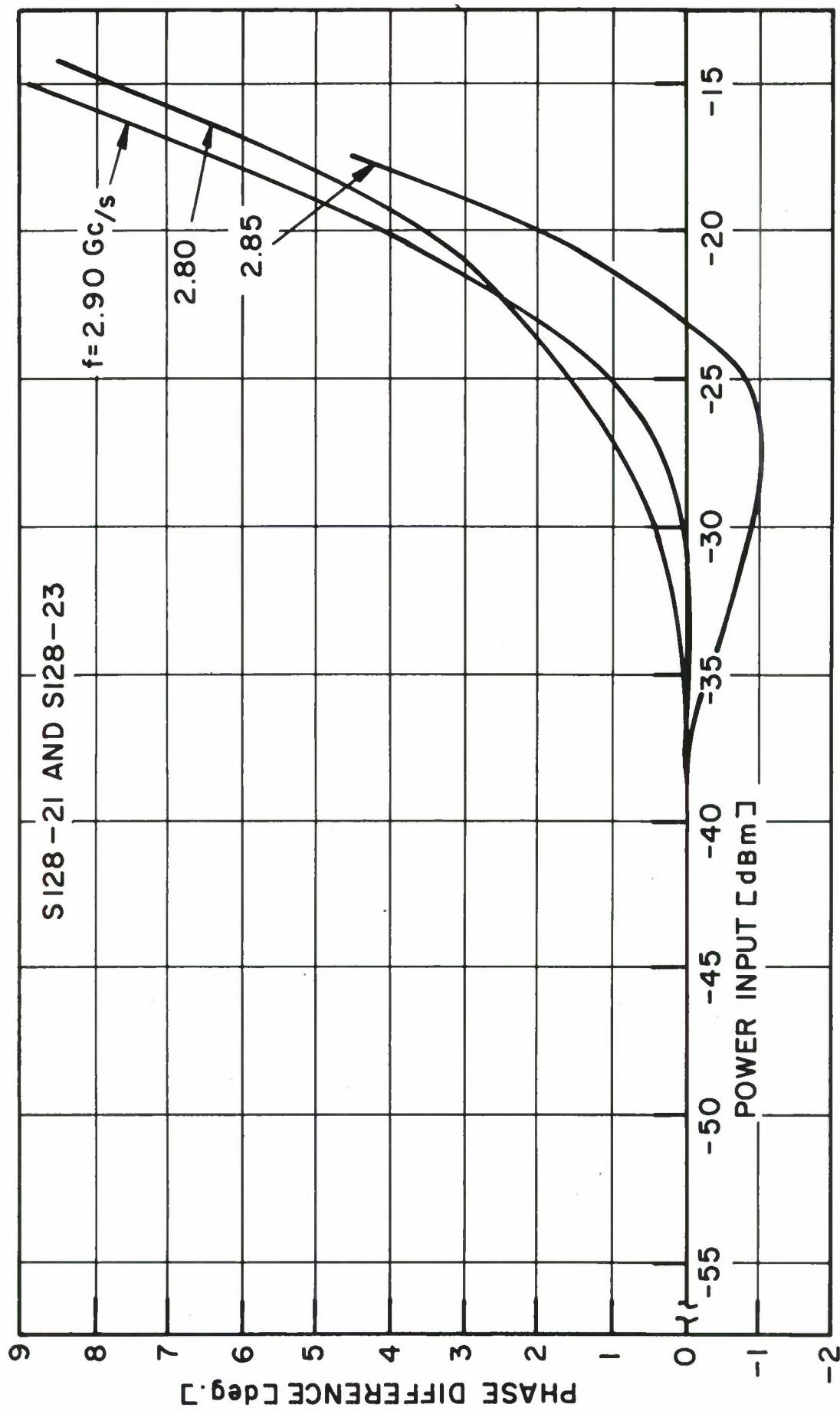
FIG. 44 PHASE TRACKING vs. POWER INPUT
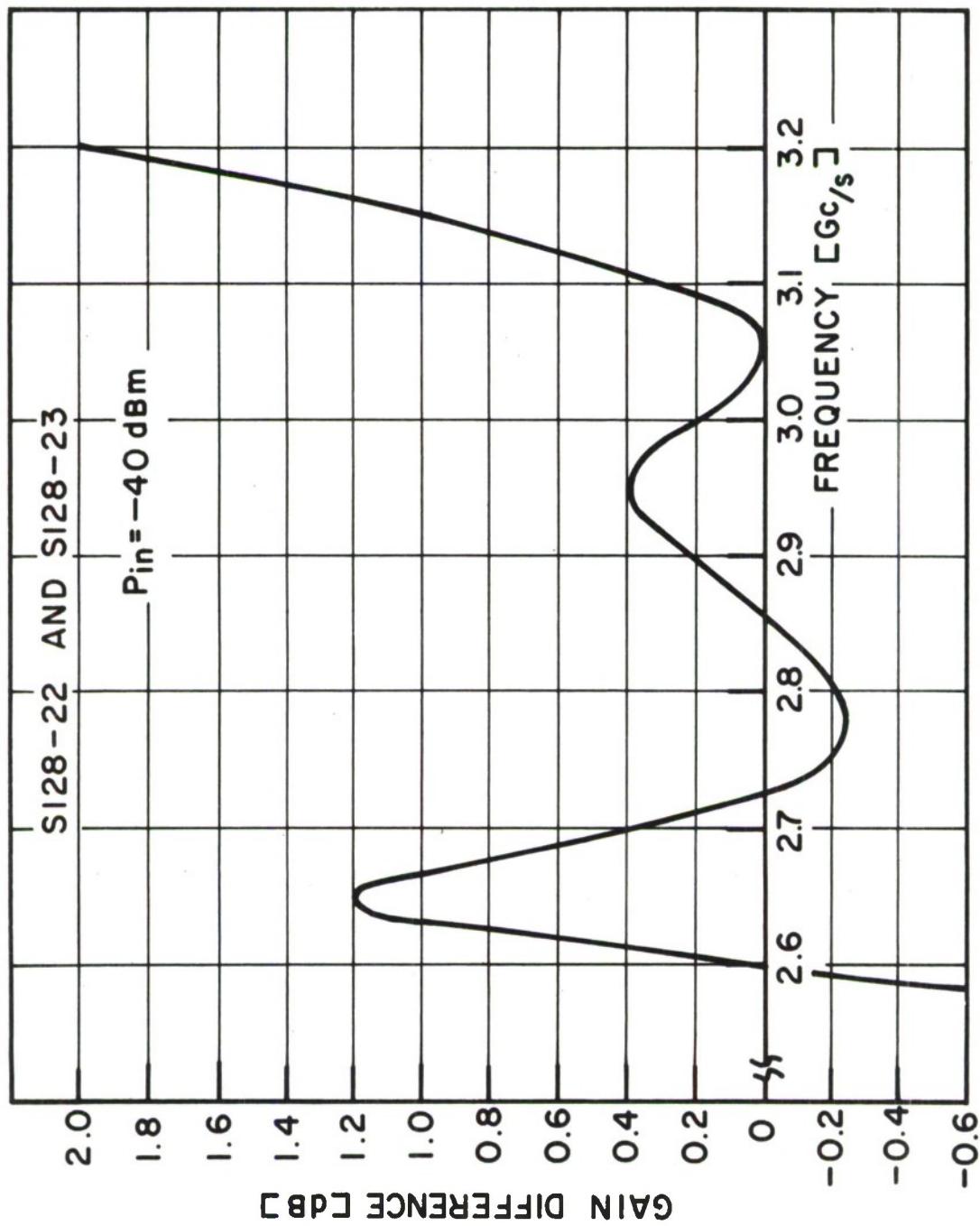
FIG. 45 AMPLITUDE TRACKING vs. FREQUENCY
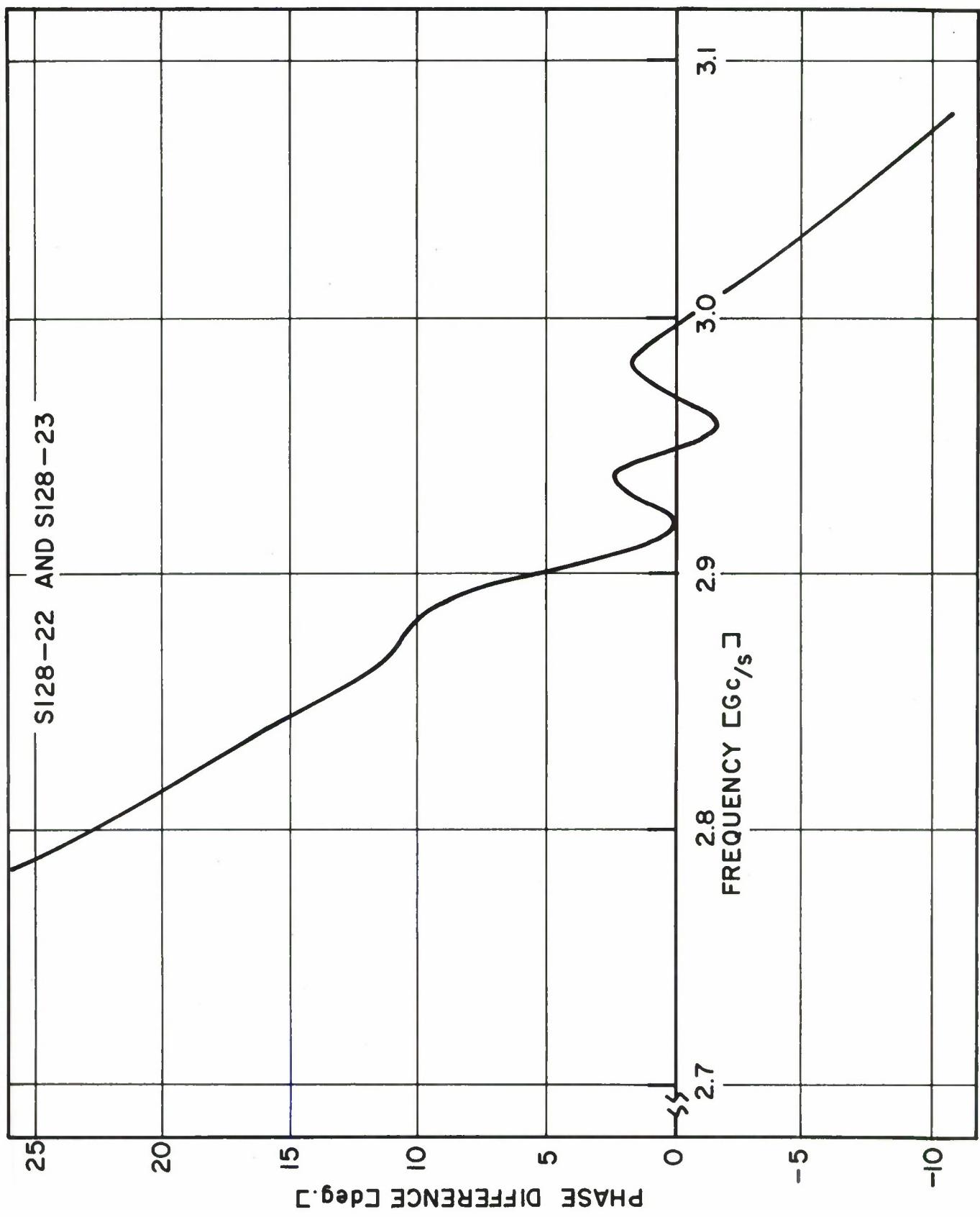
FIG. 46 PHASE TRACKING vs. FREQUENCY
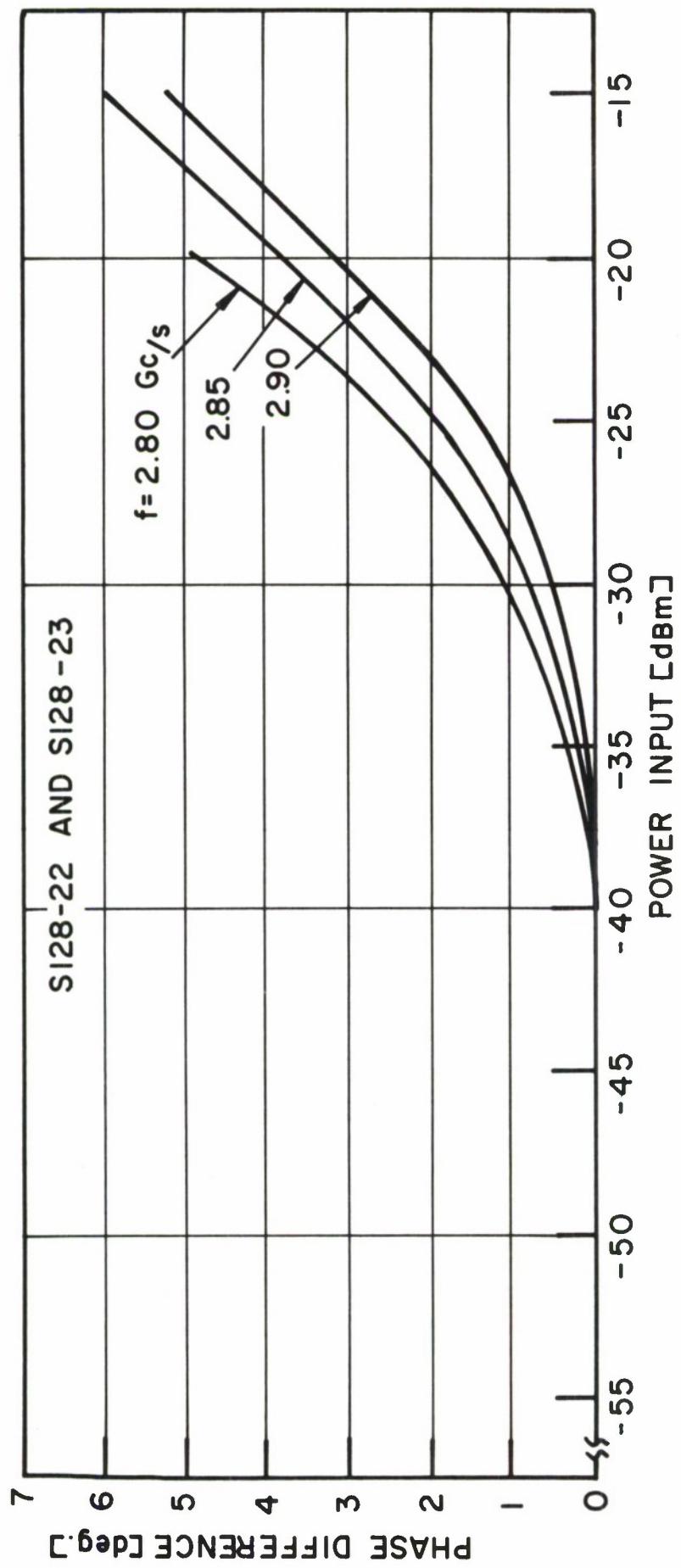
FIG. 47 PHASE TRACKING vs. POWER INPUT

# DOCUMENT CONTROL DATA - R&D

*(Security classification of title, body of abstract and indexing annotation must be entered when the overall report is classified)*

| 1. ORIGINATING ACTIVITY (Corporate author) | 2a. REPORT SECURITY CLASSIFICATION |
|---|---|
| Radio Corporation of America under Subcontract No. 305 to Lincoln Laboratory, M. I. T. | Unclassified |
| | 2b. GROUP None |

**3. REPORT TITLE**

Development of a Large Dynamic Range Tunnel Diode Amplifier for Phased Array Receivers

**4. DESCRIPTIVE NOTES** *(Type of report end inclusive dates)*

Subcontract Report

**5. AUTHOR(S)** *(Last name, first name, initial)*

Presser, Adolph and Sterzer, Fred

| 6. REPORT DATE | 7a. TOTAL NO. OF PAGES | 7b. NO. OF REFS |
|---|---|---|
| 1 January to 30 September 1965 | 83 | 9 |

| 8a. CONTRACT OR GRANT NO. AF 19 (628)-500 | 9a. ORIGINATOR'S REPORT NUMBER(S) |
|---|---|
| b. PROJECT NO. | Final Report |
| c. None | 9b. OTHER REPORT NO(S) *(Any other numbers that may be assigned this report)* |
| d. | ESD-TDR-65-592 |

**10. AVAILABILITY/LIMITATION NOTICES**

None

| 11. SUPPLEMENTARY NOTES | 12. SPONSORING MILITARY ACTIVITY |
|---|---|
| None | Air Force Systems Command, USAF |

**13. ABSTRACT**

The objectives of this two-phase program was to develop large dynamic range S-band tunnel diode amplifiers for phased array receivers. Under phase 1 a prototype amplifier was developed and subsequently delivered to Lincoln Laboratory. Phase II called for a reproducibility study of these amplifiers, and for the investigation of amplifier characteristics pertinent to phased array applications.

This report covers the experimental work performed under phase II and the results that were obtained in reproducing three amplifiers. Also, for completeness of this report, parts of the theoretical work performed during phase I are included.

Three two-stage tunnel diode amplifiers were delivered to Lincoln Laboratory in fulfillment of the phase II requirements. These amplifiers operate at a center frequency of $2.85\,Gc/s \pm 2\%$, have a 1.5 dB bandwidth ranging from 400-450 Mc/s at a gain of 18.0 to 18.5 dB, and have a noise figure between 5.6 and 5.9 dB. The amplifiers are unconditionally stable, and their output power at the 1 dB compression point ranges from $-10.5\,dBm$ to $-12\,dBm$. The phases of any two amplifiers track within $\pm 3°$ over a band of 110-190 Mc/s, and the amplitudes track within $\pm 1/2\,dB$ over a Band of 290-410 Mc/s.

**14. KEY WORDS**

tunnel diode amplifier
phased array receivers